UCSF
UC San Francisco Electronic Theses and Dissertations

Title
A yeast screen for PI3K inhibitor resistance

Permalink
https://escholarship.org/uc/item/7jq9j87d

Author
Zunder, Eli Richard

Publication Date
2008

Peer reviewed|Thesis/dissertation

eScholarship.org Powered by the California Digital Library
University of California

A yeast screen for PI3K inhibitor resistance

by

Eli Richard Zunder

DISSERTATION

Submitted in partial satisfaction of the requirements for the degree of

DOCTOR OF PHILOSOPHY

in

Biophysics

in the

GRADUATE DIVISION

of the

UNIVERSITY OF CALIFORNIA, SAN FRANCISCO

Copyright © 2009

by

Eli Richard Zunder

To Barbara and Noah, with love

Acknowledgements

There are many people that I need to thank for helping me with this work. First of all I would like to thank Kevan Shokat, for letting me join his lab and for supporting me throughout my graduate career. I am continually amazed at how he can run a large and very successful lab of almost twenty graduate students and postdocs, and still often seem to know my own project better than I know it myself. I couldn't ask for a better role model: I am inspired not only by his breadth of knowledge and enthusiasm for science, but also by his sense of humor and his ability to balance everything he does for the lab along with his family life. I will try to follow his example, and I'll consider myself lucky if I am half as successful in science and in life.

Doing research in the Shokat lab has been a real pleasure. I could list names of graduate students and postdocs I'd like to thank for advice and conversation, but it would basically be the entire lab. I hope that my next lab will have the same spirit of friendliness and generosity. Also, I need to thank Valerie Ohman for everything she does to keep our lab running smoothly, because she does the hard work that makes our lives easy, and I need to thank Julie Ransom and Rebecca Brown for keeping me on track in the Biophysics program.

Much of the work in this dissertation is reproduced from the following publication: Zunder et al. Cancer Cell. 2008 Aug 12;14(2):180-92. Kevan Shokat is listed as the corresponding author; he directed and supervised this research. Zachary Knight, Benjamin Houseman, and Beth Apsel are also listed as co-authors on this publication. Their contributions to the work are as follows: Zachary Knight synthesized the

compounds PIK-90, PIK-93, PI-103, and PIK-75, and also provided invaluable advice at all stages of the PI3K resistance screen project. He is the driving force behind the Shokat lab's foray into PI3K signaling, and my experiments would not have been possible without the very strong foundation that he laid. Benjamin Houseman synthesized the compound PW-12 as well as additional quantities of PIK-90, and Beth Apsel synthesized PP-110. Besides the synthesis of these PI3K inhibitors, all other experiments described in the Cancer Cell paper, as well as the rest of this dissertation, were performed exclusively by me, Eli Zunder.

I did receive reagents and assistance with protocols from several people that I need to thank here: Karl Kulcher provided the drug-sensitized YRP1 strain; Chao Zhang and Jen Snead assisted me with yeast culture techniques; Yi Liu at Intellikine provided the inhibitor BEZ-235; Dorothea Fiedler, Assen Roguev, and Nevan Krogan provided assistance with the Virtek colony arrayer; Sohye Kang and Peter Vogt provided p110αH1047R containing plasmids; Brandon Tavshanjian provided assistance with generation of the MCF10A cell lines; and Jeffrey Henise and Jack Taunton provided the pcDNA3-EcoR/MCAT1 vector. This work was supported by the Howard Hughes Medical Institute.

Finally I would like to thank my family. To my parents in Vermont, Phil and Marj, thank you for everything in my life. To my sister Rachel and her boyfriend Jaime at Berkeley, thanks for always coming over to visit and for humoring me by talking about science. To my wife Barbara, thank you for loving me and for putting up with life as a "lab widow." And finally to my son Noah, thanks for letting us sleep at night most of the time, and for all the fun that we're going to have together.

Abstract

A yeast screen for PI3K inhibitor resistance

by Eli Richard Zunder

Drug resistance is a seemingly inescapable fact in cancer therapy. This is particularly true for anti-cancer protein kinase inhibitors, which can be remarkably successful, but inevitably fall victim to resistance – leading to patient relapse. The most frequent mechanism of resistance is mutations in the target protein kinase that preclude inhibitor binding, and the discovery and characterization of these mutations has led to second generation kinase inhibitors that can overcome the initial drug-resistant mutations. The related PI3K inhibitors show much promise as anti-cancer therapy, but are likely to be just as susceptible to drug resistance by mutation of the target kinase. The oncogenic PI3K isoform p110α is the most frequently mutated kinase in human cancer, and numerous drugs targeting this kinase are currently in pre-clinical development or early stage clinical trials. Clinical resistance mutations appear likely, but currently none have been reported. Using a S. cerevisiae screen against a structurally diverse panel of PI3K inhibitors, I have identified a potential hotspot for resistance mutations (Ile 800), a drug-sensitizing mutation (Lys814Cys), and a surprising lack of resistance mutations at the gatekeeper residue (Ile 848). The screening protocol described here is applicable to several other drug targets that inhibit S. cerevisiae growth in addition to p110α, and hopefully will be used as part of a broader trend in drug development to predict drug-resistant mutations in the laboratory rather than waiting for them to occur in patients, in order to accelerate the development of second-generation inhibitors.

Table of Contents

Acknowledgements iv

Abstract vi

Table of Contents vii

List of Figures xi

List of Tables xiv

1 The identification of p110α as a drug target for anti-cancer therapy 1

1.1 Introduction 1

1.2 The PI3K family of kinases 2

1.2.1 Phosphatidylinositol and phosphoinositides in the mammalian cell 2

1.2.2 Organization and substrate specificities of the PI3K family 5

1.3 Discovery of PI3K and its role in cancer 8

1.3.1 Identification of PI3K activity and its correlation with retroviral oncogenic transformation 8

1.3.2 Identification of p110α as an oncogene 9

1.3.3 Roles for the other p110 isoforms in cancer 11

1.4 PI3K inhibitor development 12

1.4.1 The first PI3K inhibitors: wortmannin and LY294002 12

1.4.2 Isoform-selective PI3K inhibitors 13

1.4.3 PI3K inhibitors currently in clinical trials 15

1.5 Similarities and differences between the PI3K and protein kinase families 16

1.5.1 Sequence and structural alignment 16
1.5.2 The gatekeeper residue 19
1.6 Conclusion 25
2 A S. cerevisiae assay for PI3K activity and inhibition 27
2.1 Introduction 27
2.2 PI3K-induced toxicity in S. cerevisiae 29
2.3 Rescue of PI3K-induced toxicity by potent and selective PI3K inhibitors 30
2.3.1 Advantages of the drug-permeablized strain YRP1 31
2.3.2 Reverse Halo Assays 33
2.4 Mutagenesis of the p110α gatekeeper 34
2.5 Pursuit of an alternative screening strategy: growth rescue by PI3K activity 36
2.5.1 CDC25ts rescue by PH domain-Ras fusion protein and PI3K activity 37
2.5.2 Growth rescue by additional p110 isoforms 38
2.5.3 PI3K inhibitors do not inhibit growth rescue by p110β-CAAX 39
2.5.4 Modulation of PH-Ras system by introduction of PTEN, p85α, and multiple p110 isoforms 41
2.6 Materials and Methods 43
2.6.1 Yeast strains 43
2.6.2 Yeast plasmids 43
2.6.3 Yeast transformation 44
2.6.4 Reverse Halo Assay 45
2.6.5 PI3K inhibitors 46
2.7 Conclusion 46

3 A mutagenic screen in S. cerevisiae for PI3K inhibitor resistance 47
3.1 Introduction 47
3.2 Library Generation 48
3.2.1 NNK mutagenesis and YRP1 transformation 49
3.3 Robotic 384-pin format library replication and image analysis 50
3.4 Active site residues' tolerance to mutation 51
3.5 PI3K inhibitor screen 53
3.6 Identification of drug-resistant and drug-sensitized p110α mutations 54
3.7 Screen hit serial dilution growth assays 55
3.8 Materials and Methods 56
3.8.1 Screen Outline 56
3.8.2 NNK mutagenesis and library creation 57
3.8.3 YRP1 transformation, robotic pinning, drug screen, and image analysis. 58
3.8.4 Structural Analysis 58
3.9 Conclusion 59
4 Extension of yeast screen hits 61
4.1 Introduction 61
4.2 In vitro kinase assays 61
4.3 MCF10A transformation 63
4.4 Materials and Methods 70
4.4.1 Plasmids 70
4.4.2 In vitro PI3K kinase assays 71
4.4.3 MCF10A culture and transformation assays 72

4.4.4 Creation of p110α-expressing MCF10A cell lines 72
4.4.5 MCF10A EGF-independent transformation assays 73
4.4.6 MCF10A western blotting 73
4.5 Conclusion 74
Bibliography 77

List of Figures

Figure 1.1. Chemical structures of phosphatidylinositol and high abundance phosphoinositides 3

Figure 1.2. Chemical structures of low abundance phosphoinositides 4

Figure 1.3. Flow chart of the steps of phosphoinositide synthesis in mammalian cells 6

Figure 1.4. X-ray crystal structure of p110α in complex with the iSH2 domain of p85α . 7

Figure 1.5. p110α hot spot mutations identified in human cancer 10

Figure 1.6. Chemical structures of the first PI3K inhibitors: quercetin, wortmannin, and LY294002 12

Figure 1.7. Mechanism of PI3K inactivation by wortmannin 13

Figure 1.8. Chemical structures of the isoform-selective inhibitors TGX-221 (p110β), IC87114 (p110δ), and AS-605240 (p110γ) 14

Figure 1.9. Chemical structures of PI3K inhibitors that target p110α 15

Figure 1.10. Sequence alignment of the PI3K and protein kinase families 17

Figure 1.11. Sequence homology of the PI3K and protein kinase families 18

Figure 1.12. Structural alignment of p110γ and c-Src bound to the dual PI3K-protein kinase inhibitor S1 19

Figure 1.13. Wild type and analog-sensitive protein kinase bound to PP1 and 1-NM-PP1, respectively 22

Figure 1.14. Position of the gatekeeper residue in PI3K and protein kinases 23

Figure 1.15. Sequence alignment of p110α with protein kinases in which gatekeeper drug-resistance mutations are observed 24

Figure 1.16. Distribution of residues at the gatekeeper position in the human PI3K and protein kinase families 24

Figure 1.17. Ile 848 and the PI3K affinity pocket 25

Figure 2.1. Phosphoinositide synthesis in S. cereviaise 29

Figure 2.2. Rescue of PI3K-induced growth inhibition in S. cerevisiae by selective PI3K inhibitors 32

Figure 2.3. Reverse halo assays with YRP1 overexpressing p110αH1047R-CAAX 33

Figure 2.4. p110α gatekeeper mutant serial dilutions 35

Figure 2.5. S. cerevisiae growth rescue by PI3K activity 37

Figure 2.6. Growth rescue by the p110β, p110α, and p110δ isoforms 38

Figure 2.7. CDC25ts PH-Ras PI3K halo assays 40

Figure 2.8. Introduction of PTEN and p85α into the CDC25ts PH-Ras PI3K growth rescue system 42

Figure 3.1. Affinity pocket residues chosen for saturation mutagenesis 48

Figure 3.2. Sequence alignment of the human PI3K family 49

Figure 3.3. DNA sequencing chromatograms of the p110α mutagenic libraries 49

Figure 3.4. Growth inhibition profile of a representative NNK libary in the YRP1 strain 50

Figure 3.5. Tolerance to mutation in the p110α affinity pocket 51

Figure 3.6. Structural representation of tolerance to mutation in the p110α affinity pocket 52

Figure 3.7. Representative images and the corresponding colony size distributions of a pooled active mutant library 54

Figure 3.8. Representative plates showing the characterization of yeast screen hits by serial dilution analysis..... 55

Figure 3.9. 1:3 Serial dilutions of the most promising drug-resistant (I800M) and drug-sensitized (L814C) strains..... 55

Figure 3.10. S. cerevisiae Screen Outline 56

Figure 4.1. Kinase activity of p110α screen hit mutants 62

Figure 4.2. Altered inhibitor sensitivities of the p110α screen hit mutants 62

Figure 4.3. GFP signal relative to side scatter observed during MCF10A FACS sorting 64

Figure 4.4. EGF-independent growth of MCF10A cell lines expressing oncogenic p110α with drug resistant or sensitizing mutations..... 65

Figure 4.5. Altered in vivo inhibitor sensitivities of the resistance mutants I800L and I800M..... 66

Figure 4.6. Altered in vivo inhibitor sensitivities of the drug-sensitized mutant L814C 67

Figure 4.7. Akt/PKB signaling downstream of drug-resistant and drug-sensitized p110α mutants..... 68

Figure 4.8. Akt/PKB signaling in respone to PI3K inhibitors 69

List of Tables

Table 1.1. Phosphoinositide composition of the plasma membrane of selected mammalian cell types 3

Table 1.2. Phosphoinositide levels in insulin stimulated fat and muscle cells 4

Table 1.3. PI3K inhibitors in clinical trials as cancer therapy 16

Table 2.1. Oligonucleotide primers used for subcloning p110α and site-directed mutagenesis 44

Table 3.1. Inhibitor concentrations used in the p110α mutant screen 53

Table 3.2. Primers used for saturation mutagenesis 57

Table 4.1. Oligonucleotide primers used for subcloning p110α 71

1 The identification of p110α as a drug target for anti-cancer therapy

1.1 Introduction

p110α is a class IA phosphoinositide 3-kinase (PI3K) that phosphorylates phosphatidylinositol-(4,5)-bisphosphate (PtdIns-4,5-P_2) at the D-3 position of its inositol ring, generating phosphatidylinositol-(3,4,5)-trisphosphate (PtdIns-3,4,5-P_3) [1]. PtdIns-3,4,5-P_3 recruits downstream signaling proteins such as Akt/PKB to the plasma membrane, leading to increased growth, proliferation, motility, and cell survival [1]. p110α has attracted considerable interest as a drug target [2-4] since its identification as an oncogene [5] and the discovery of activating point mutations in its encoding gene *PIK3CA* [6]. In the absence of p110α mutation, other PI3K pathway members, including Receptor Tyrosine Kinases (RTKs), Ras, Phosphatase and Tensin Homolog (PTEN), and Akt/PKB are frequently mutated instead [7-9], highlighting the critical role PI3K signaling plays in oncogenesis and tumor maintenance [10, 11]. Mounting evidence for the importance of PI3K signaling in cancer has spurred the development of PI3K-targeted

small molecule inhibitors, several of which are now entering clinical trials as cancer therapy [12, 13].

1.2 The PI3K family of kinases

1.2.1 Phosphatidylinositol and phosphoinositides in the mammalian cell

Phosphatidylinositol (PtdIns) is a relatively minor component of the plasma membrane and other lipid membranes in the mammalian cell, but it is unique among phospholipids in that it can be phosphorylated at multiple positions, including the D-3, D-4, and D-5 hydroxyls of its polar inositol head group. These phosphorylated PtdIns derivatives are termed phosphoinositides. In addition to influencing the biophysical properties of cellular membranes due to their additional bulk and negative charge, these phosphoinositides can also act as second messengers in signal transduction pathways that regulate growth, proliferation, survival, cytoskeletal organization, vesicle trafficking, ion channel function, and nutrient transport in mammalian cells.

The mammalian plasma membrane is approximately 30%-40% lipid by dry weight ; of these lipids, 50 – 75% are phospholipids, and 2 – 15% of these phospholipids are PtdIns [14-17]. The three most abundant species of PtdIns in mammalian cells include the unphosphorylated form, as well as the phosphoinositides phosphatidylinositol-(4)-phosphate (PtdIns-4-P) and phosphatidylinositol-(4,5)-bisphosphate (PtdIns-4,5-P_2), representing approximately 90% of the total PtdIns species [18].

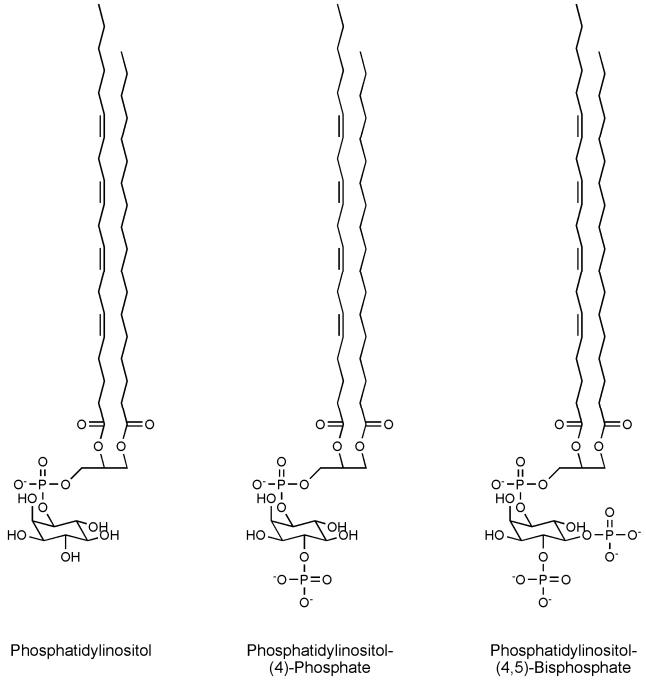

Figure 1.1. Chemical structures of phosphatidylinositol and high abundance phosphoinositides.

Phosphoinositide species	Cell Type		
	Erythrocytes	Platelets	Lymphoma
PI	1.9 ± 0.7	4.5 ± 0.9	5.8 ± 0.9
PI-4-P	0.9 ± 0.4	0.9 ± 0.4	0.1 ± 0.2
PI-4,5-P_2	1.5 ± 0.4	0.4 ± 0.2	0.3 ± 0.3

Table 1.1. Phosphoinositide composition of the plasma membrane of selected mammalian cell types [19]. Values are shown as mol % total phospholipid, ± 1 standard deviation (SD).

In addition to PtdIns, PtdIns-4-P, and PtdIns-4,5-P_2, several other phosphoinositide species exist in mammalian cell membranes at relatively low concentrations. These low abundance species include phosphatidylinositol-(3)-phosphate (PtdIns-3-P), phosphatidylinositol-(3,4)-bisphosphate (PtdIns-3,4-P_2), phosphatidylinositol-(3,5)-

bisphosphate (PtdIns-3,5-P_2), and phosphatidylinositol-(3,4,5)-trisphosphate (PtdIns-3,4,5-P_3).

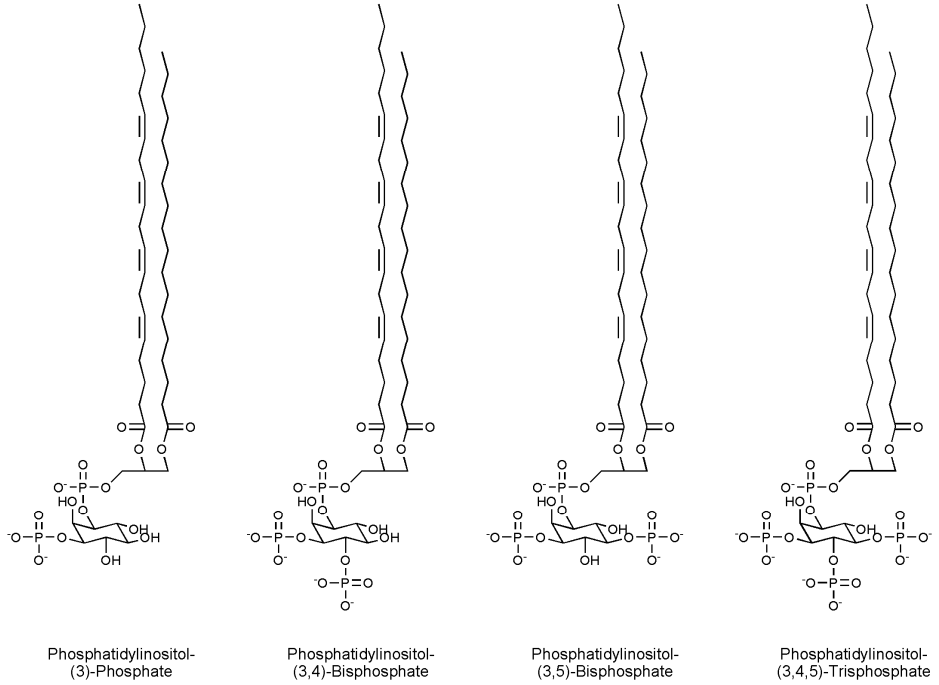

Figure 1.2: Chemical structures of low abundance phosphoinositides

Phosphoinositide species	Cell Type			
	L1 adipocytes		L6 myotubes	
	no insulin	100nM insulin	no insulin	100nM insulin
PtdIns-3-P	1.21	1.27	0.72	0.72
PtdIns-3,4-P_2	0.09	0.52	not done	not done
PtdIns-3,5-P_2	0.31	0.34	0.20	0.24
PtdIns-3,4,5-P_3	0.19	0.35	0.05	0.17

Table 1.2. Phosphoinositide levels in insulin stimulated fat and muscle cells [20]. Phosphoinositide levels are reported as % PtdIns-4,5-P_2, which remains relatively constant. Measurements were taken after 10 minutes of insulin stimulation.

The concentration of each phosphoinositide species helps determine the membrane's biophysical properties, and also controls signal transduction in the cell. Phosphoinositides can modulate the activity of membrane proteins such as ion channels

and transporters [21], serve as substrates for phospholipases such as phospholipase C (PLC) to generate diacyl glycerol (DAG) and soluble inositol-(1,4,5)-trisphosphate (IP_3) [22, 23], or act as docking sites that recruit downstream signaling proteins to the plasma membrane [24]. Because the concentration of each phosphoinositide species is critical to cellular function, the production and degradation of each species is tightly regulated by phosphoinositide kinases and phosphatases, respectively.

1.2.2 Organization and substrate specificities of the PI3K family

Synthesis of the multiple phosphoinositide species present in mammalian cells is governed in large part by the phosphoinositide kinases of the PI3K family, which is classified by sequence homology to include the Class I, Class II, and Class III PI3Ks, the phosphatidylinositol-(4)-kinases (PI4Ks), and the phosphoinositide-3-kinase-related protein kinases (PIKKs). In addition to PI3Ks and PI4Ks, which phosphorylate the inositol head group on the D-3 and D-4 positions, respectively, cellular phosphoinositide levels are also regulated by the evolutionarily divergent phosphatidylinositol-phosphate-(4)-kinase (PIP4K) and phosphatidylinositol-phosphate-(5)-kinase (PIP5K), by phosphatases such as PTEN and Src homology 2 domain-containing inositol 5' phosphatase (SHIP), and by phospholipases such as phospholipase C (PLC).

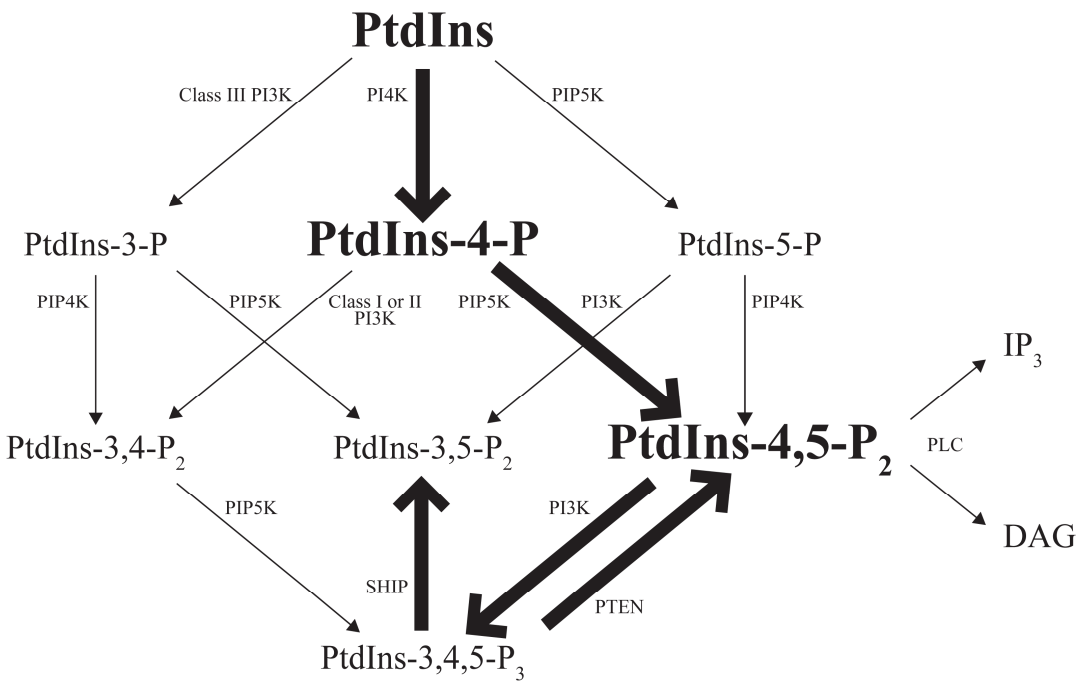

Figure 1.3. Flow chart of the steps of phosphoinositide synthesis in mammalian cells [18]. The bold text indicates high abundance PtdIns species, and the bold arrows indicate the dominant pathways with respect to Class I PI3K signaling.

Class I PI3Ks are thought to preferentially phosphorylate PtdIns-4,5-P_2 as a substrate in vivo, producing PtdIns-3,4,5-P_3 [25]. Class I PI3Ks are heterodimers consisting of a catalytic subunit of approximately 110 kD and a regulatory subunit. The catalytic subunits are further divided into Class IA and Class IB. The Class IA PI3K catalytic subunits, p110α, p110β, and p110δ, associate with regulatory subunits p85α, p85β, p55α, p55γ, and p50α, all of which contain dual Src homology 2 (SH2) domains that target the Class IA PI3Ks to phosphotyrosine residues on activated receptor tyrosine kinases (RTKs) and associated adaptor proteins [26, 27]. The only known Class IB PI3K catalytic subunit is p110γ, and it primarily associates with the regulatory subunit p101 [28], although recent studies suggest another possible Class IB regulatory subunit: $p84/p87^{PIKAP}$ [29, 30]. Class IB PI3Ks are activated by the βγ subunits of heterotrimeric

G proteins downstream of G-protein coupled receptors (GPCRs), rather than by phosphotyrosine residues on RTKs or adaptor proteins [31]. Recent evidence has shown that in addition to p110γ, p110β can also be activated by βγ subunit downstream of GPCR signaling in some circumstances [32], although unlike p110γ, it requires phosphotyrosine in addition to the βγ subunit for activation. In addition to activation by RTKs or GPCRs, all Class I PI3Ks can bind to activated Ras protein through the Ras binding domain (RBD) present in each catalytic subunit, providing an additional mechanism for activation [33].

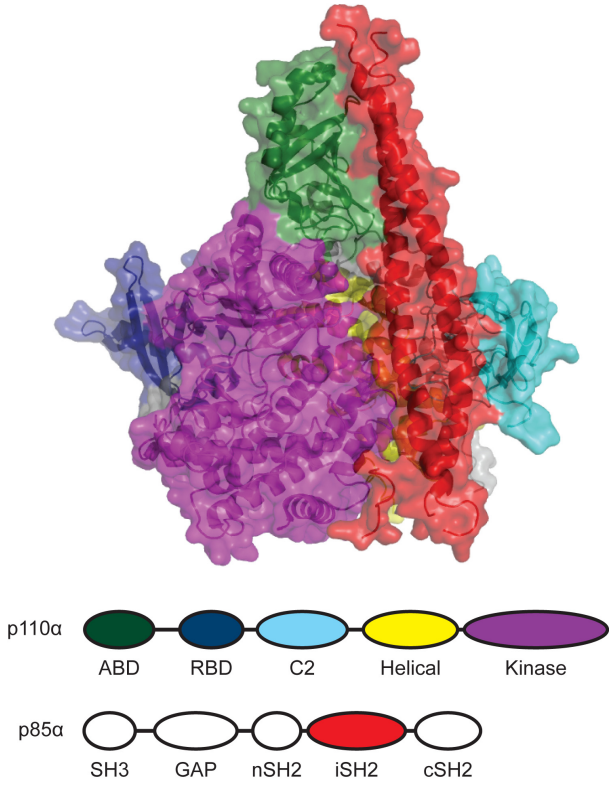

Figure 1.4. X-ray crystal structure of p110α in complex with the iSH2 domain of p85α [34]. ABD = adaptor binding domain (p85 interacting), RBD = Ras binding domain, SH3 = src homology 3 domain, GAP = Rho GTPase Activating Protein homology domain (inactive), nSH2 = N-terminal src homolgy 2 domain, iSH2 = inter-SH2 domain, cSH2 = C-terminal src homology 2 domain. The p110α domain structure is representative of Class IA PI3Ks, Class IB domain structure is identical except it has no ABD domain.

The Class II PI3Ks PI3KC2α, PI3KC2β, and PI3KC2γ are able to phosphorylate PtdIns and PtdIns-4-P in vitro [35], but their preferred in vivo substrate and their biological function remain elusive [36]. The Class III PI3K vps34 can only phosphorylate PtdIns to produce PtdIns-3-P, which regulates endocytic trafficking, nutrient sensing, and autophagy in mammalian cells [37]. The PI4Ks in the PI3K family, PI4Kα and PI4Kβ, phosphorylate PtdIns to produce PtdIns-4-P, one of the major species of phosphoinositide in the cell that can go on to be further phosphorylated by other phosphoinositide kinases to yield PtdIns-3,4-P_2 and PtdIns-4,5-P_2, respectively, feeding into other signaling pathways. The PIKKs in the PI3K family, ATM, ATR, SMG1, mTOR, and DNAPK, do not display any detectable lipid kinase activity, and rather act as Ser/Thr kinases, but they are targeted by many of the same kinase inhibitor classes due to their sequence homology with the PI3Ks.

1.3 Discovery of PI3K and its role in cancer

1.3.1 Identification of PI3K activity and its correlation with retroviral oncogenic transformation

PI3K activity was first observed in association with the oncogenic tyrosine kinases $pp60^{v\text{-}src}$ and $pp68^{v\text{-}ros}$ from rous sarcoma virus (RSV) and avian sarcoma virus UR2, respectively [38, 39]. Subsequent studies found that PI3K activity also associated with polyoma middle T/$pp60^{c\text{-}src}$ and with the PDGF receptor [40-42]. In vitro, this kinase activity could phosphorylate PtdIns, PtdIns-4-P, and PtdIns-4,5-P_2 [43], but kinetic analysis of the formation of PtdIns-3-P, PtdIns-3,4-P_2, and PtdIns-3,4,5-P_3 in intact cells

after ^{32}P labeling indicates that PtdIns-4,5-P_2 is the primary physiological substrate for PI3K, producing PtdIns-3,4,5-P_3 as its primary physiological product [25]. Initially, phosphoinositide and tyrosine phosphorylation were thought to result from a single kinase, because the two activities were tightly associated biochemically, and were inhibited in parallel in mammalian cells. However, subsequent studies demonstrated that phosphorylation of tyrosine residues and phosphoinositides were due to separate kinase activities: transformation-defective polyoma mutants with reduced associated PI3K activity but intact tyrosine kinase activity were identified [41], and the two activities were separated biochemically using high salt and detergent conditions [44]. A 85 kD protein, the p85 regulatory subunit, was observed to correlate with PI3K activity [42], and the heterodimeric PI3K complex containing the p85 regulatory subunit and the p110 catalytic subunit was purified [45] and cloned [26, 46].

1.3.2 Identification of p110α as an oncogene

PI3K activity has been strongly correlated with oncogenic transformation since it was discovered, because mutants of polyoma middle T, $pp60^{v\text{-}src}$ and of $pp130^{gag\text{-}abl}$ that failed to associate with PI3K activity lost the ability to transform cells [40-42, 47-49]. In these cases, PI3K acts downstream of an oncogenic tyrosine kinase, but later experiments in Chicken Embryo Fibroblasts (CEFs) identified the PI3K catalytic isoform p110α as an oncogene itself that can drive transformation when membrane localized and overexpressed [5]. The discovery of activating point mutations in p110α [6] underlined the importance of PI3K signaling in human cancer, as it is the most frequently mutated oncogene in breast (27%) and endometrial (22%) cancers, and is the second most

frequently mutated oncogene behind Ras in colon cancer (23%). p110α is mutated in 15% of all tumors sequenced, making it the most frequently mutated kinase in human cancer (frequencies obtained from the Wellcome Trust Sanger Institute Cancer Genome Project, http://www.sanger.ac.uk/genetics/CGP).

More than 80% of reported p110α mutations are confined to the helical domain mutations E542K and E545K, and the kinase domain mutation H1047R [6].

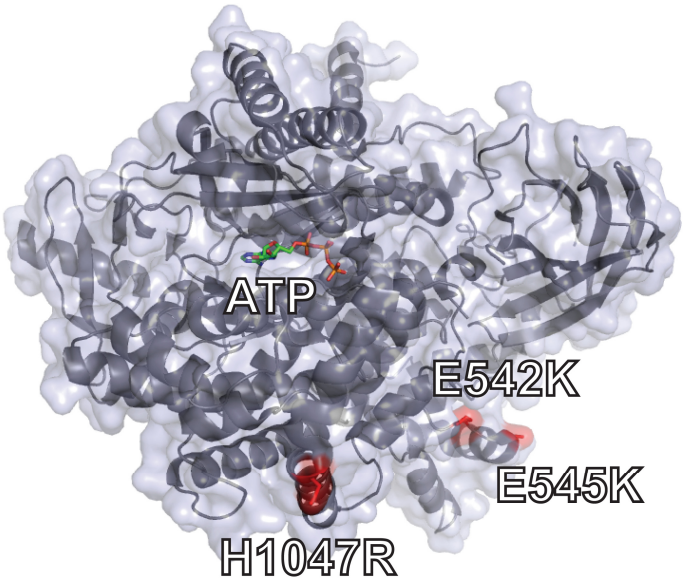

Figure 1.5. p110α hot spot mutations identified in human cancer.

These mutants exhibit increased catalytic activity [6, 50] and are capable of transforming a number of cell lines in tissue culture and xenograft models [50-54]. The exact mechanism how these mutants activate p110α is not clear, but biochemical experiments and structural modeling indicate that the helical domain mutations E542K and E545K disrupt a salt bridge critical for the inhibitory interaction with the nSH2 domain of the p85 regulatory subunit [55]. Experiments combining the three p110α hot spot mutations with ABD and RBD mutations that disrupt binding to the p85 regulatory subunit and to

Ras, respectively, show that the helical domain mutants E542K and E545K require Ras-GTP but not p85 binding for activation, while the kinase domain mutant H1047R requires p85 binding but not Ras-GTP [56].

1.3.3 Roles for the other p110 isoforms in cancer

No cancer specific mutations have been found in the p110 isoforms besides p110α, but it is possible they could act as oncogenes by overexpression rather than by mutation. This is suggested by experiments in CEFs that show overexpression of p110β, p110δ, and p110γ induced oncogenic transformation [57], but this result is not replicated with p110β in human mammary epithelial cells [51], suggesting that CEFs may be more permissive for transformation by PI3K activity than human cells.

While it is unclear whether p110 isoforms besides p110α can drive transformation in human cancer, mounting evidence suggests they play an indispensible role in several cancer types, either as oncogenes themselves, or more likely as key downstream mediators of a transformation-driving oncogenic lesion. p110β, rather than p110α, has been shown to be essential for ERBB2-driven mammary gland tumorigenesis [58], growth of PTEN-deficient cancer cell lines [59, 60], and prostate tumorigenesis driven by PTEN loss [61]. The importance of p110β in cancer driven by PTEN loss is explained by experiments that indicate p110β provides a constant basal PI3K activity, while p110α is normally low, but provides an acute spike in PI3K activity after growth factor stimulation [20]. Therefore, while p110β appears "silent" in response to growth factors, it becomes a "powerhouse" to drive oncogenic transformation in the absence of PTEN [61].

p110δ and p110γ are expressed primarily in leukocytes of the immune system, and therefore are not frequently linked with cancer in non-immune tissues. p110δ has been shown to be required for proliferation and survival of acute myeloid leukemia (AML) cells [62, 63], and p110γ may play a role in chronic myeloid leukemia (CML) [64], although unlike the p110δ AML result which uses the highly p110δ-specific inhibitor IC87114 [65] for validation, the p110γ CML result relies on overexpressing a dominant-negative kinase-dead p110γ for validation, and therefore may not be as reliable.

1.4 PI3K inhibitor development

1.4.1 The first PI3K inhibitors: wortmannin and LY294002

Quercetin was the first small molecule identified as a PI3K inhibitor [66], but it is not specific for the PI3K family as it inhibits several protein kinases as well [67-71]. The first specific PI3K family inhibitors identified were the fungal metabolite wortmannin and the synthetic small molecule LY294002 [72].

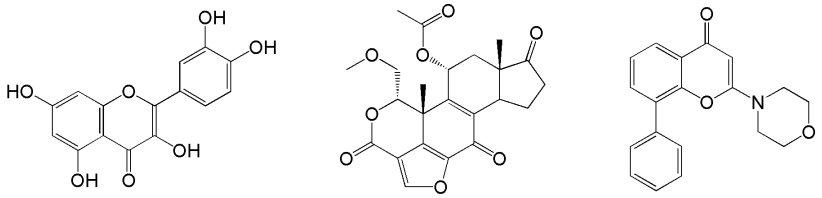

Quercetin Wortmannin LY294002

Figure 1.6. Chemical structures of the first PI3K inhibitors: quercetin, wortmannin, and LY294002

The natural product wortmannin was first identified as an antibiotic produced by the fungus *Penicillium wortmanni* [73], and was later identified as a PI3K inhibitor [74] based on its disruption of agonist-mediated respiratory burst in neutrophils [75], and then shown to broadly inhibit the PI3K family [76]. LY294002 was identified by medicinal chemistry efforts to improve the selectivity of quercetin for the PI3K family [72]. Wortmannin and LY294002 are relatively specific for the PI3K family over protein kinases, but both are broadly active within the PI3K family [20], including the PIKK protein kinases [76, 77]. Wortmannin is highly potent as it is an irreversible inhibitor that covalently modifies the catalytic lysine of PI3K family members, and LY294002 is weakly potent, with IC_{50}s in the μM range for PI3K family members.

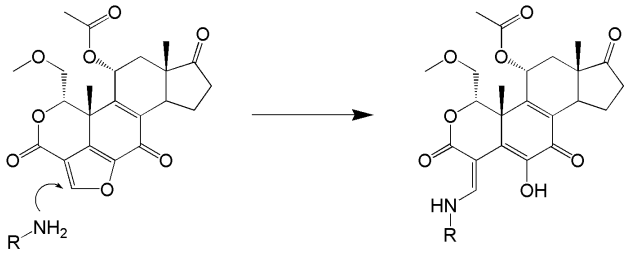

Figure 1.7. Mechanism of PI3K inactivation by wortmannin. The nucleophilic Lysine 802 in p110α attacks the furan ring of wortmannin, resulting in a stable PI3K-wortmannin adduct.

Although both wortmannin and LY294002 lack specificity within the PI3K family, they have both been invaluable tools for the study of PI3K signaling.

1.4.2 Isoform-selective PI3K inhibitors

Mounting evidence for the importance of PI3K signaling in cancer [78] as well as autoimmune and inflammatory disease [79], has led to a surge in the development of isoform-specific PI3K inhibitors, in the hopes of increased potency and decreased off-

target effects. Inhibitors selective for p110β (TGX-221) [80], p110δ (IC87114) [65], and p110γ (AS-605240) [81, 82] have been identified by medicinal chemistry efforts, but p110α-selective inhibitors remain elusive.

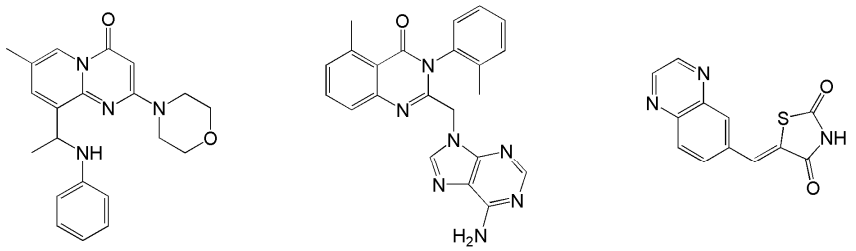

TGX-221 IC87114 AS-605240

Figure 1.8. Chemical structures of the isoform-selective inhibitors TGX-221 (p110β), IC87114 (p110δ), and AS-605240 (p110γ).

Potent inhibitors have been identified that are selective for p110α among the p110 isoforms: PI-103 and PIK-75 are approximately 5-fold and 10-fold selective, respectively, but these compounds have significant off-target effects. PI-103 potently inhibits mTOR in addition to p110α [83], and PIK-75 potently inhibits a number of protein kinase targets [20]. Other PI3K inhibitors that potently target p110α include PIK-90, PIK-85, PIK-93, PW-12, PP-110, and BEZ-235 [20, 84-86].

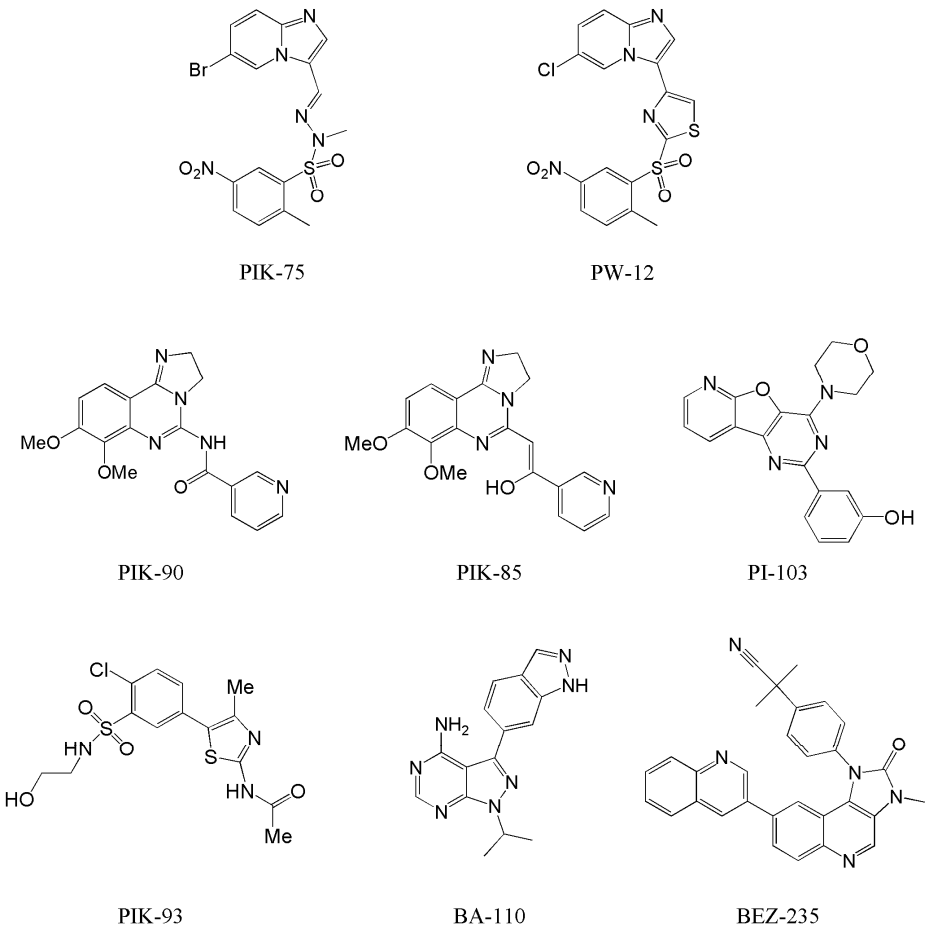

Figure 1.9. Chemical structures of PI3K inhibitors that target p110α

Although no single inhibitor is completely selective for p110α, the use of multiple PI3K inhibitors with varied p110 targets has allowed biological functions to be attributed to p110α by inference [20].

1.4.3 PI3K inhibitors currently in clinical trials

Several PI3K inhibitors have entered clinical trials for cancer therapy against several tumor types.

Study Start Date	Compound	Company	Conditions	Phase
Dec 2006	BEZ-235	Novartis	Solid Tumors, Breast Cancer	I
Jun 2007	XL765	Exelixis	Cancer	I/II
Jun 2007	XL147	Exelixis	Cancer	I/II
Dec 2007	BGT226	Novartis	Solid Tumors, Breast Cancer, Cowden Syndrome	I
Jun 2008	PX-866	ProlX	Advanced Solid Tumors	I
Jun 2008	CAL-101	Calistoga	Chronic Lymphocytic Leukemia (CLL), Lymphoma, Non-Hodgkin (NHL), Acute Myeloid Leukemia (AML)	I
not disclosed	GDC-0941	Piramed / Genentech	Locally Advanced or Metastatic Solid Tumors	I
not disclosed	SF1126	Semafore	Advanced or Metastatic Tumors	I

Table 1.3. PI3K inhibitors in clinical trials as cancer therapy

1.5 Similarities and differences between the PI3K and protein kinase families

1.5.1 Sequence and structural alignment

While the PI3K family shares the same two-lobe kinase domain structure and catalytic sequence motifs of the protein kinase family, the two families are evolutionarily divergent. Sequence homology between PI3K and protein kinases is so low that a sequence alignment of the two families was not possible until the x-ray crystal structure of p110γ was solved, allowing for a structure-based sequence alignment [87]. Even with structural information, the alignment is only possible in the region of highest conservation, in the N-lobe of the kinase domain between the P-loop motif and the DFG motif, because outside this region the structures diverge significantly.

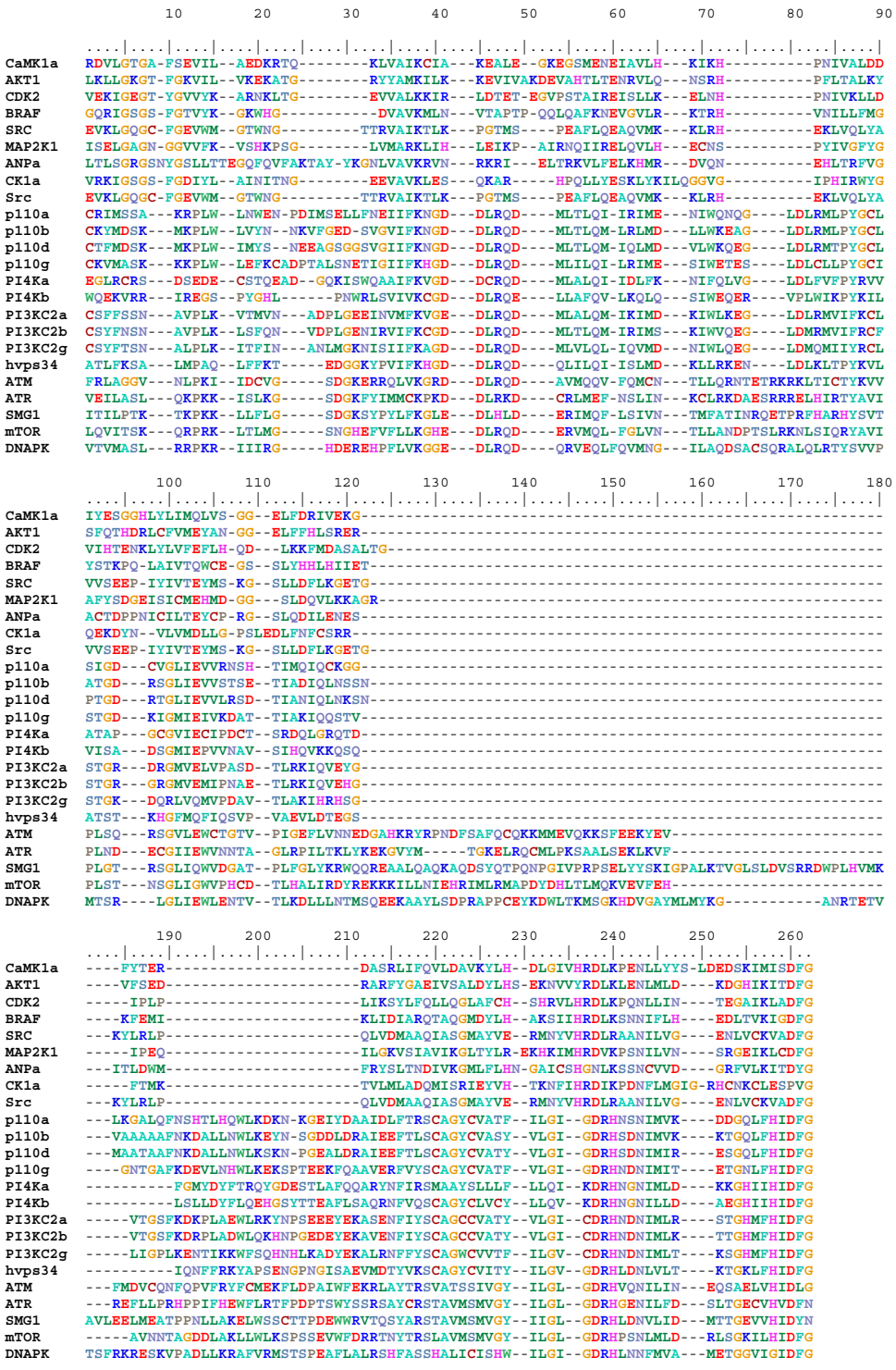

Figure 1.10. Sequence alignment of the PI3K and protein kinase families. The alignment includes representative protein kinases from each of the 8 major protein kinase groups: AGC (AKT1), CAMK (CAMK1a), CMGC (CDK2), CK1 (CK1A), RGC (ANPA), STE (MEK1), TKL (BRAF), and TK (CSRC). Amino acids are colored to highlight conservation of properties: red = negative charge, blue = positive charge, green = aliphatic, etc.

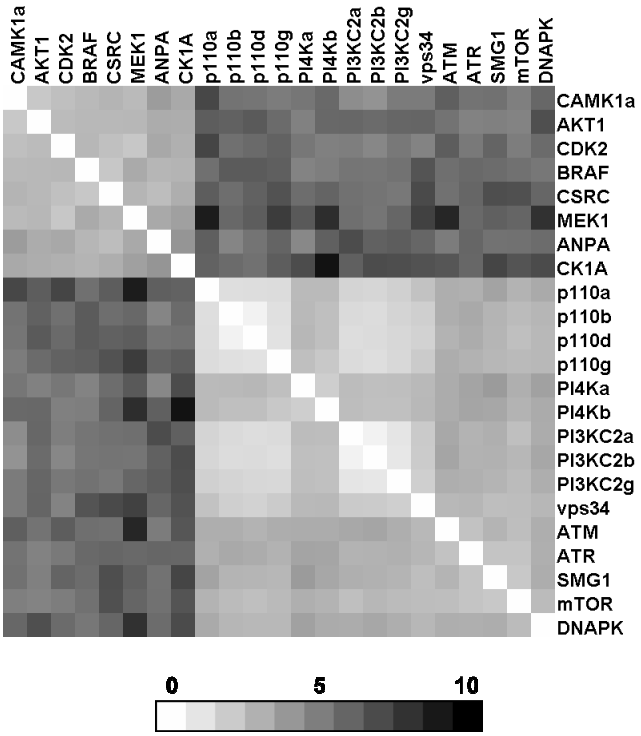

Figure 1.11. Sequence homology of the PI3K and protein kinase families. Pairwise protein distance values were calculated for the segment between the P-loop and DFG using the PAM matrix, and then normalized to a 0-10 scale, where 0 is identical and 10 is highest divergence.

The PI3K and protein kinase families are evolutionarily divergent, differing in primary sequence and tertiary structure, and in the vast majority of cases, PI3K inhibitors do not inhibit protein kinases and vice versa. However, extensive screening efforts have identified a dual PI3K-protein kinase inhibitor scaffold [85].

Figure 1.12. Structural alignment of p110γ and c-Src bound to the dual PI3K-protein kinase inhibitor S1 [85]. p110γ = green, and c-Src = purple.

1.5.2 The gatekeeper residue

Protein kinases play a key role in signal transduction in eukaryotic cells, relaying changes in the cell's environment, such as nutrient availability or the presence of growth factors, into a functional change in the cell's behavior, such as metabolism, growth, and proliferation. Because practically every cellular process is controlled by protein kinase signaling at some level, the study of individual protein kinases and their biological function promises a far greater understanding of cellular biology. Interrogation of individual protein kinases by genetic methods such as gene knock-outs or RNAi is not ideal however, because these methods work on the hour to day timescale, but changes in protein kinase signaling occur rapidly, often on the second and minute timescale. Another disadvantage is that gene knock-out and RNAi remove the entire protein from

the cell, which is very different from simply removing the kinase activity, because the protein may contain additional domains with enzymatic activity or scaffolding function, although this concern is allayed by the knock-out/knock-in kinase-dead strategy. These two disadvantages, timescale and complete protein loss, often confound the results of genetic experiments on protein kinase signaling. The long delay allows the cell to adapt, often by upregulating compensatory pathways and masking the kinase's true role in cellular signaling, and the loss of the entire protein can lead to changes independent of protein kinase activity [88].

Small molecule protein kinase inhibitors are therefore preferable to genetic methods for the study of signal transduction, because they can rapidly inhibit their target on the second to minute timescale, and they leave the target protein intact so that it can maintain any kinase-independent function. Additional advantages of small molecule protein kinase inhibitors over genetic techniques are rapid washout and the ability to titrate kinase inhibition, both of which are impossible with genetic knock-outs and highly difficult with RNAi. Finally, there is a great practical advantage to studying protein kinase signaling with small molecule inhibitors, because many kinase inhibitors are successful drugs used to treat human disease, and kinase inhibition is an active area of research for the pharmaceutical industry. Therefore, studying kinase inhibition with small molecule inhibitors rather than genetic techniques better mimics the effect of a potential drug, which is often the desired outcome in biomedical and translational studies.

For all the advantages of small molecule inhibitors over genetic techniques, there is one disadvantage for the study of kinase signaling: specificity. While genetic knock-out of a kinase is 100% specific, and the specificity of RNAi can be validated easily with

multiple constructs, small molecule kinase inhibitors are inherently non-specific, because the active sites of every kinase are highly similar, and therefore difficult for a potent small molecule to distinguish between. In addition to the greater than 500 possible kinases for off target effects, ATP-competitive kinase inhibitors may also inhibit any of the numerous ATPases in the cell. Recent efforts have identified kinase inhibitors that gain specificity by targeting unique inactive conformations [89, 90], or allosteric sites distant from the active site [91, 92], but the majority of kinase inhibitors used in basic science and clinical applications target the ATP binding site, and therefore inhibit a large number of kinases in addition to their primary target [93].

The non-specificity of kinase inhibitors is most troubling because it is never completely defined: it is impossible to test a small molecule for inhibition of every enzymatic activity in the cell. Currently, a popular measure of specificity of small molecule kinase inhibitors is performed by screening against kinase panels that number in the hundreds [85, 93], and these panels are constantly increasing in size as additional kinase assays are developed. Another excellent measure of kinase inhibitor specificity is by affinity purification of targets by the small molecule inhibitor immobilized onto a solid resin [94, 95]. Differences in cellular protein levels over several orders of magnitude can make low abundance targets difficult to identify by affinity chromatography.

An ingenious solution to the problem of kinase inhibitor selectivity has been the development of a chemical-genetic method to generate mutant kinases that are uniquely inhibited by a modified kinase inhibitor that, due to introduced steric bulk, does not inhibit any other kinase [96]. This analog-sensitive “bump-hole” strategy, using space-

creating mutations in the kinase active site and "bumped" inhibitors, takes advantage of a conserved active site residue termed the gatekeeper residue, which is present in all human protein kinases, but is never an alanine or glycine. Most protein kinases tolerate mutation of the gatekeeper residue to alanine or glycine without significant loss of activity, creating a larger active site pocket that can be uniquely inhibited by "bumped" inhibitors such as 1-napthylmethyl-PP1.

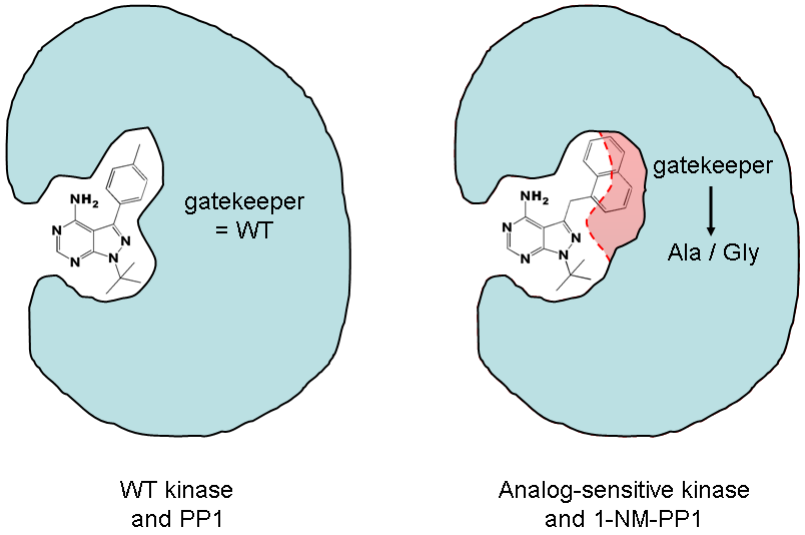

Figure 1.13. Wild type and analog-sensitive protein kinase bound to PP1 and 1-NM-PP1, respectively. The space created by the gatekeeper Ala/Gly mutation is indicated in red, illustrating the steric clash that prohibits 1-NM-PP1 from binding to all WT protein kinases.

The analog-sensitive strategy is well suited to studying protein kinases in S. cerevisiae and mice due to the ease in which WT protein kinase can be replaced with an analog-sensitive mutant genetically [96, 97]. Replacing the endogenous WT kinase with the analog-sensitive mutant is more difficult in human cells, but can be accomplished by RNAi-mediated knock-down of the endogenous kinase targeted against non-coding regions of the mRNA, coupled with simultaneous expression of the mutant kinase by transfection or retroviral infection, or by homologous gene replacement with a

recombinant adeno-associated virus (rAAV) strategy [98-100]. In addition to selective inhibition experiments, analog-sensitive mutant kinases can also be used for substrate labeling, in order to identify direct kinase substrates [101-103].

In addition to its usefulness for the creation of analog-sensitive protein kinase alleles, the gatekeeper residue is also the most frequent site of drug-resistant mutations in protein kinases that are targeted by small molecule inhibitors as cancer therapy, including imatinib (BCR-ABL, KIT, PDGFR) and gefitinib/erlotinib (EGFR) [104], due to its conserved position at a critical site for inhibitor binding and its relative tolerance to mutation.. Many drug-resistant mutations decrease kinase activity in addition to inhibitor binding, but the gatekeeper resistance mutations retain high kinase activity, and are also the most difficult of all resistance mutations against which to identify selective second generation inhibitors [105].

Compared to protein kinases, the gatekeeper residue occupies a similar position in the PI3K active site, as seen in the p110γ and p110α x-ray crystal structures [34, 87].

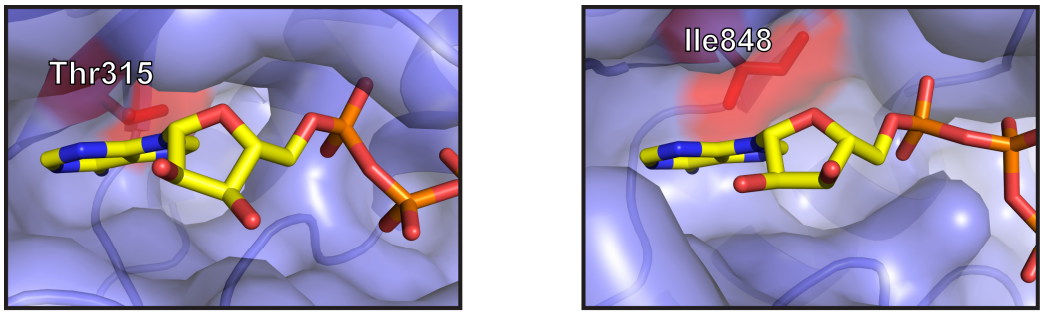

Figure 1.14. Position of the gatekeeper residue in PI3K and protein kinases. ATP is shown bound to Abl (PDB code 2G1T) and p110α (PDB code 2RD0). ATP from the p110γ cocrystal (PDB code 1E8X) was overlaid onto p110α (PDB code 2RD0) by structural alignment. The gatekeeper residue in each protein is labeled and highlighted in red.

Unlike the protein kinases susceptible to drug-resistant mutations, p110α and the other p110 isoforms have an Ile residue at the gatekeeper position rather than a Thr residue.

```
Abl(311-319)     F Y I I T E F M T
c-Kit(666-674)   T L V I T E Y C C
PDGFR(670-678)   I Y I I T E Y C F
EGFR(786-794)    V Q L I T Q L M P
p110α(844-852)   C V G L I E V V R
```

Figure 1.15. Sequence alignment of p110α with protein kinases in which gatekeeper drug-resistance mutations are observed. The gatekeeper position is highlighted with a black box.

Attempts to generate analog-sensitive p110α mutants have been unsuccessful, because mutation of the gatekeeper residue Ile 848 to either Ala or Gly results in a complete loss of catalytic activity [106]. This may be due to reduced tolerance to mutation at the PI3K gatekeeper position relative to protein kinases, which is suggested by the distribution of residues from each family, with protein kinases able to accommodate most residues but the PI3K family only containing the aliphatic residues Ile, Leu, Met, and Val.

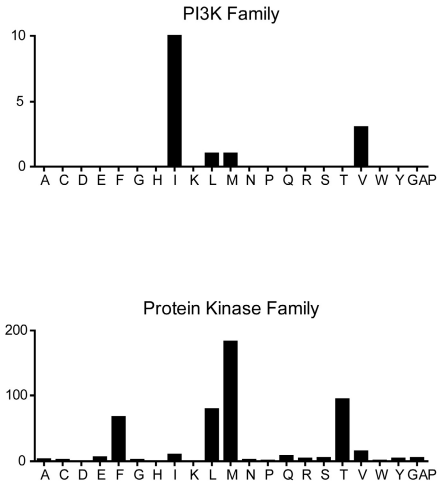

Figure 1.16. Distribution of residues at the gatekeeper position in the human PI3K and protein kinase families.

However, structural analysis suggests that mutation of Ile 848 to a larger residue would block access to the "affinity pocket" [20] that is accessed by the most potent PI3K inhibitors but not by ATP, and therefore the gatekeeper residue may be a likely site of drug-resistant mutations to anti-cancer PI3K inhibitors that are now entering clinical trials.

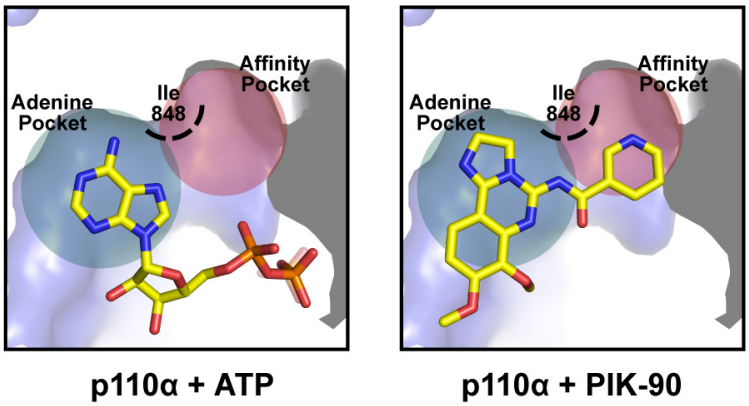

Figure 1.17. Ile 848 and the PI3K affinity pocket. The x-ray crystal structure of p110α (PDB code 2RD0) is overlaid with ATP and PIK-90 from p110γ co-crystal structures (PDB codes 1E8X and 2CHX, respectively). The adenine pocket is colored green, the affinity pocket is colored red, and the location of Ile 848 is indicated by a dashed line.

1.6 Conclusion

PtdIns can be phosphorylated to several species of phosphoinositides that play an important role as second messengers in cellular signal transduction. PtdIns-3,4,5-P_3 generated by PI3K activity plays an important role in cancer signaling, and the catalytic isoform p110α is one of the most frequently mutated oncogenes in human cancer. The development of potent and selective PI3K inhibitors has greatly improved our knowledge of PI3K biology. Many of these PI3K inhibitors are entering clinical trials, but it is likely they will be susceptible to resistance mutations in a similar manner to protein kinase

inhibitors. Structural similarities between the PI3K and protein kinase active sites suggest that the gatekeeper residue Ile 848 of the oncogenic PI3K isoform p110α is likely to be a potential site for drug-resistant mutations.

2 A S. cerevisiae assay for PI3K activity and inhibition

2.1 Introduction

The identification and characterization of protein kinase resistance mutations from cancer patients has led to the development of effective second generation inhibitors [105, 107, 108]. Remarkably, resistance screens in mammalian tissue culture are able to reproduce these mutations in vitro [109-111]. Typically in these screens the cells are grown in the presence of drug to select for resistance mutations, either starting with the drug at sub-lethal concentration and slowly increasing over each cell passage, or holding the concentration constant at a level that kills the majority of the cells immediately. The experiment may rely on the genetic diversity already present in the cell line used, or it may rely on the resistance mutation spontaneously occurring as the cells grow and proliferate. Alternatively, genetic diversity may be introduced by culturing the cells in the presence of a mutagen such as N-ethyl N-nitrosourea (ENU), or by mutagenizing the DNA of the target kinase in vitro with error-prone PCR or E. coli strains deficient in

DNA repair, before introducing the mutant library retrovirally into the cell line for screening.

Screening for drug resistance in mammalian tissue culture has proven successful in many examples, but there are several drawbacks to note. One drawback is the difficulty in recovering and identifying the mutation that confers resistance. The target gene, either endogenous or retrovirally integrated, must be recovered from the genomic DNA and sequenced, and this is complicated by multiple copies in the genome: two for endogenous genes in diploid organisms, and possibly more for retroviral insertions. Additionally, the cell line's drug resistance may not be due to a mutation in the target kinase of interest, but instead may be due to any number of mechanisms, including overexpression of the target kinase, increased expression of drug-efflux pumps, or upregulation of alternative pathways that compensate for inhibition of the target kinase. Much can be learned by studying these unique drug-resistant cell lines, but tracking down the source of resistance can be quite difficult, and most drug resistance studies to not follow up these cell lines after it is determined that the target kinase in not mutated. Another drawback is that mammalian screens cannot find drug resistance mutations in a single target kinase if the drug being used has multiple targets, each of which is essential for growth and proliferation, such as the dual PI3K-mTOR inhibitor PI-103 [83]. Finally, a significant drawback to screening for drug resistance in mammalian tissue culture is the difficulty in scaling the screen up to include a large number of inhibitors.

In order to identify PI3K drug-resistant mutations, I developed an assay for PI3K inhibition in S. cerevisiae that overcomes these limitations of mammalian tissue culture screens. Unlike mammalian cells, the recovery of DNA from S. cerevisiae is rapid and

straightforward by plasmid rescue. S. cerevisiae has no endogenous PI3K activity and selective PI3K inhibitors do not inhibit growth, so off-target mechanisms of drug-resistance are minimized. PI3K inhibitors that target multiple human kinases that would confound a mammalian screen are amenable to study in S. cerevisiae, because the additional targets are simply not present. Finally, using S. cerevisiae allows an unlimited number of drug conditions to be screened via replica plating or robotic pinning. This is essential because the structural diversity of PI3K inhibitors in clinical development [13] suggests that a different spectrum of resistance mutations may arise against each inhibitor, and I sought to identify p110α resistance mutations before they occur in cancer patients, with no prior knowledge of clinical resistance in the PI3K family, and uncertainty about which PI3K inhibitor will make it through clinical trials as a successful anti-cancer therapy.

2.2 PI3K-induced toxicity in S. cerevisiae

While S. cerevisiae expresses several lipid kinases in the PI3K family and produces several species of phosphoinositide, it lacks an endogenous p110 homolog, and therefore does not produce PtdIns-3,4,5-P_3 [112].

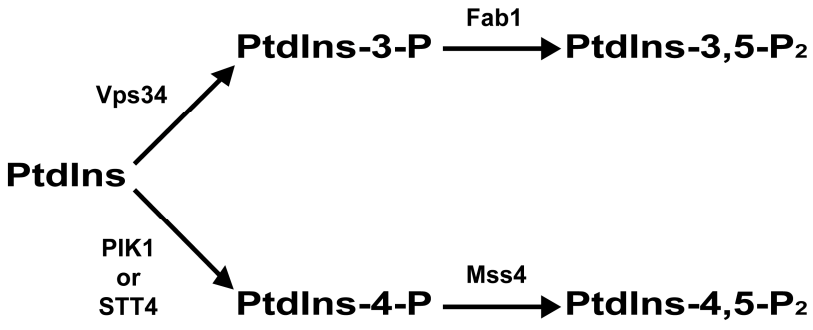

Figure 2.1. Phosphoinositide synthesis in S. cerevisiae.

Previous studies have shown that overexpression of membrane-localized p110α-CAAX inhibits S. cerevisiae growth [113, 114]. This growth inhibition could be caused either by an inherent toxicity of PtdIns-3,4,5-P_3 that S. cerevisiae cannot degrade, or by depletion of PtdIns-4,5-P_2 and other phosphoinositides which are required in S. cerevisiae to maintain proper actin [115] and septin [116] architecture, and for membrane trafficking [112]. Activation of the cell-integrity pathway MAPK Slt2 upon induction of p110α-CAAX expression suggests that depletion of PtdIns-4,5-P_2, and subsequent disruption of actin-mediated transport of vesicles required for cell membrane and cell wall biogenesis plays a major role in the PI3K-induced growth inhibition phenotype [114].

S. cerevisiae growth inhibition is lost when p110α is overexpressed without a membrane-localizing C-terminal CAAX domain, but is partially regained if p110α is mutated from WT to the oncogenic H1047R [117]. Interestingly, growth inhibition is not partially regained with the oncogenic E545K mutant [117], perhaps because E545K is thought to activate p110α by disrupting an inhibitory interaction with the p85 regulatory subunit [55], but S. cerevisiae does not express any p85 homolog so there is no advantage for E545K in this system.

2.3 Rescue of PI3K-induced toxicity by potent and selective PI3K inhibitors

Previous studies have shown that p110α-induced growth inhibition in S. cerevisiae can be partially reversed by the low potency PI3K inhibitor LY294002 [114]; here I use a

structurally diverse panel of high potency PI3K inhibitors that completely rescue growth, taking advantage of the drug-permeablized S. cerevisiae strain YRP1.

2.3.1 Advantages of the drug-permeablized strain YRP1

In order to use PI3K-induced toxicity to study p110α inhibition in *S. cerevisiae*, I generated high copy (2μ) plasmids that express p110α-CAAX under control of a *GAL1* promoter, and transformed them into a wild-type strain AFS92 and a drug-permeablized strain YRP1 [118], which is missing the enzyme responsible for the final step of ergosterol biosynthesis (*Δerg6*), and two drug efflux pumps (*Δpdr5, Δsnq2*). Ergosterol is the yeast equivalent of cholesterol, and is an important regulator of membrane permeability and fluidity [119]. The drug efflux pumps pdr5 [120] and snq2 [121] confer resistance to antifungal agents when overexpressed, and are also able to transport kinase inhibitors out of the S. cerevisiae cell [118].

When grown on galactose, both the AFS92 and YRP1 strains expressing p110α-CAAX show greater than 1000-fold growth inhibition compared to empty vector and kinase-dead controls. PI3K-induced growth inhibition is more severe in the YRP1 strain than in the AFS92 strain, presumably because the YRP1 membrane is already weakened by the *Δerg6* mutation, and this weakness is exacerbated by PI3K-induced depletion of phosphoinositides that facilitate vesicle transport required for cell membrane and cell wall biosynthesis. Addition of the potent PI3K inhibitor PI-103 to the growth media at 5 μM only partially rescues growth of the WT strain AFS92, but it completely rescues growth of the drug-permeablized strain YRP1. Growth rescue by several other PI3K

inhibitors is more efficient in YRP1 than in AFS92 as well, and therefore the YRP1 strain was chosen for use in all further experiments.

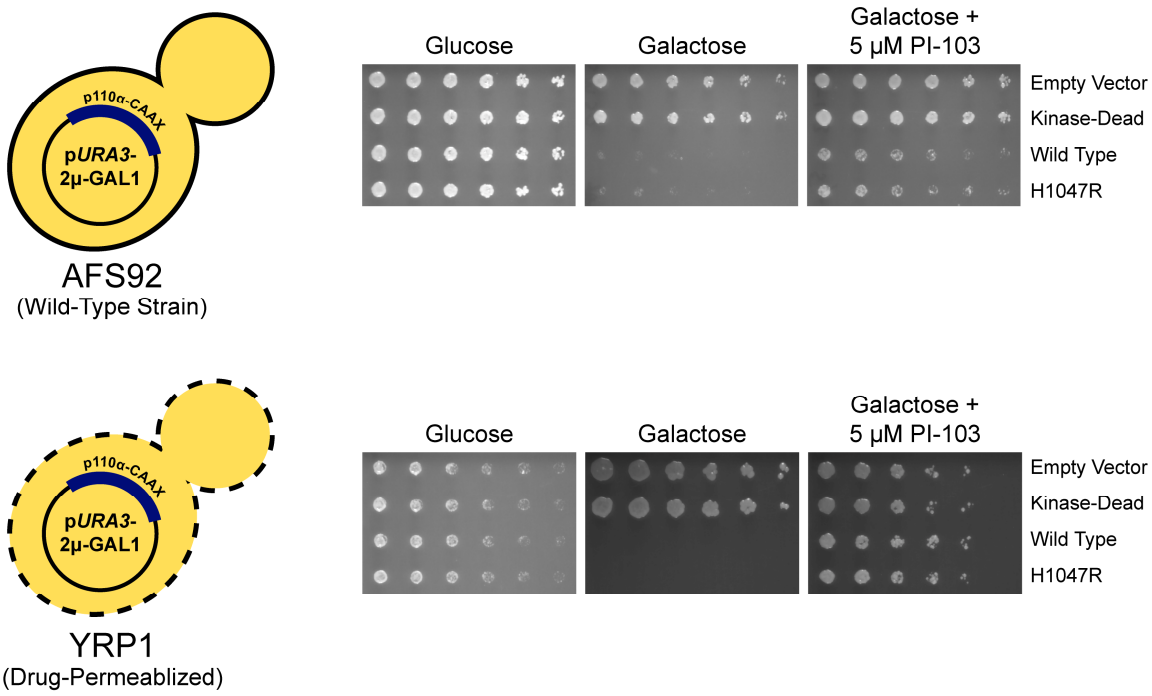

Figure 2.2. Rescue of PI3K-induced growth inhibition in S. cerevisiae by selective PI3K inhibitors. Three-fold serial dilutions of AFS92 and YRP1 yeast strains containing the pURA3-2μ-GAL1 plasmid expressing the indicated p110α-CAAX mutants were spotted onto agar plates of SD -Uracil media containing glucose, galactose, or galactose with 5 μ M PI-103. All plates were incubated at 30°C for 2 days except the YRP1 strains grown on galactose, which were incubated for 6 days.

Additionally, there is no detectable difference in growth inhibition between wild-type p110α-CAAX and the oncogenic H1047R mutant, unlike experiments with p110α without a C-terminal CAAX domain, which show that the H1047R mutation enhances growth inhibition when p110α is not membrane-localized [117].

2.3.2 Reverse Halo Assays

It was desirable to include as many diverse PI3K inhibitors as possible in the planned screen of p110α mutants, in order to identify pan-inhibitor resistance mutations as well as inhibitor-specific mutations, and to give the best chance of identifying a mutant-inhibitor pair that confers drug sensitivity. To test all PI3K inhibitors for compatibility with the yeast assay format, I used a variation on the traditional halo assay which I term "reverse halo assay." In this assay, a PI3K inhibitor is spotted onto a cellulose disc in the middle of a lawn of yeast, and instead of inhibiting growth as in a traditional halo assay, the PI3K inhibitor rescues growth, creating a "growth halo" of healthy yeast. The diameter and intensity of this halo depends on the inhibitor's potency, stability, diffusion rate, and lack of *S. cerevisiae* toxicity.

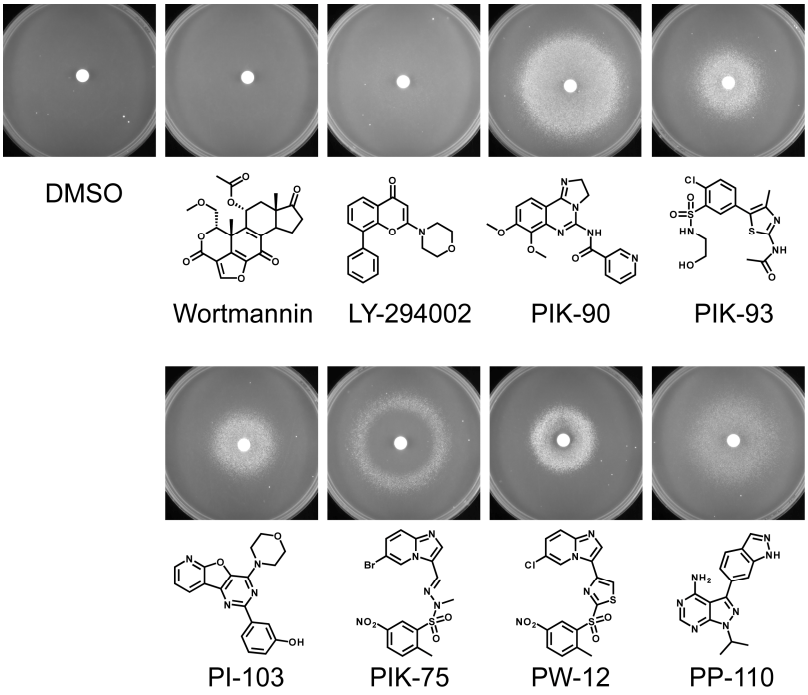

Figure 2.3. Reverse halo assays with YRP1 overexpressing p110αH1047R-CAAX. Each plate was spotted with 10 µl of a 10 mM DMSO stock of PI3K inhibitor.

Two non-selective PI3K inhibitors, wortmannin and LY294002, did not produce growth halos in the reverse halo assay. This is not surprising because wortmannin inhibits the essential *S. cerevisiae* kinase STT4 at low nM concentrations [122], while LY294002 is only a μM inhibitor of p110α and other PI3K family members [72, 76]. The imido-pyrazine PIK-75 produced only a thin ring of growth, suggesting an exceedingly narrow dose window in which a mutagenic screen could be performed. Five structurally diverse p110α inhibitors, PIK-90, PIK-93, PI-103, PW-12, and PP-110 produced growth halos of various size and intensity, indicating that these inhibitors are compatible with the S. cerevisiae assay of PI3K inhibition by growth inhibition rescue, and will work well in subsequent screens for drug-resistant p110α mutations.

2.4 Mutagenesis of the p110α gatekeeper

In my search for PI3K resistance mutations, I initially focused on the p110α gatekeeper residue, because this position is the most frequent site of drug-resistant mutations in protein kinases [104]. Using site-directed mutagenesis with randomized primers, I mutated Ile 848 to every amino acid in the low copy plasmid p*URA3*-CEN/ARS-*GAL1*-p110αH1047R-CAAX. These plasmids were transformed into YRP1, and the resulting strains were grown on either glucose or galactose to determine the relative PI3K activity of each mutant.

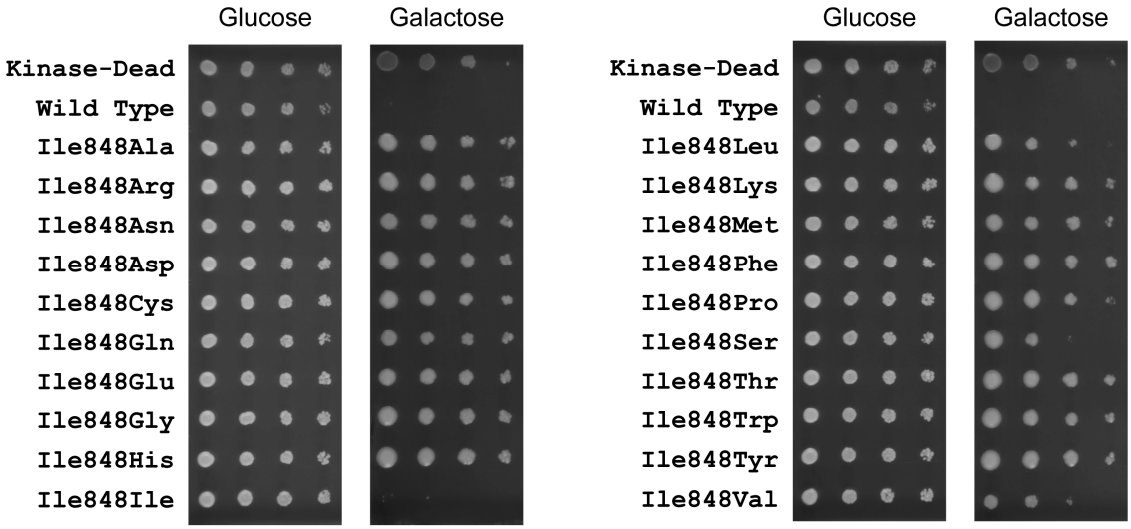

Figure 2.4. p110α gatekeeper mutant serial dilutions. The plates were incubated at 30°C for 2 days (glucose) and 6 days (galactose).

With the exception of mild growth inhibition by the conservative mutations I848L, I848S, and I848V, the other 16 p110α mutants did not inhibit yeast growth, suggesting these mutants are catalytically inactive or unstable when expressed in yeast. This result corroborates and extends previous work showing loss of catalytic activity with the I848A and I848G mutations [106]. The inability of p110α to tolerate non-conservative mutations at the gatekeeper position is reflected in the evolutionary conservation of lipid kinases at this position. Only isoleucine, leucine, methionine, and valine are found at the gatekeeper position in the PI3K family, and only isoleucine is found among the p110 isoforms, while a greater diversity of amino acid side chains is observed in the protein kinase family (Fig. 1.16).

2.5 Pursuit of an alternative screening strategy: growth rescue by PI3K activity

Screening for inhibitor resistance based on PI3K toxicity is inherently low throughput, because in order to identify a drug-resistant clone I needed to isolate a single p110α mutant-containing S. cerevisiae clone that fails to grow in the presence of PI3K inhibitor, out of a large library of p110α mutant-containing S. cerevisiae clones that grow normally in the presence of PI3K inhibitor. This can be accomplished by replica plating or robotic pinning, but performing a negative screening in this manner is orders of magnitude lower throughput than performing positive selection. The negative screen requires comparison of two plates on which PI3K activity is either induced (galactose) or repressed (glucose), and the orientation and position of each colony is critical, but with a positive selection one simply plates a lawn of mutant clones onto a single plate, and identifies the single or few colonies that were able to grow in the presence of PI3K inhibitor. With the negative screen based on PI3K-induced growth inhibition, I screened 384 clones per agar plate, but with a positive selection I could have plated 10^6 clones per agar plate, vastly increasing the number of mutant clones I could have tested per plate, and therefore reducing the amount of drug required per mutant clone to complete the screen. In this section I will describe my attempt to develop an assay in which S. cerevisiae growth is rescued by PI3K activity, and blocked by PI3K inhibitors.

2.5.1 CDC25ts rescue by PH domain-Ras fusion protein and PI3K activity

Previous studies have shown that S. cerevisiae can be made to rely on PI3K activity for growth. In this system, membrane targeted Ras complements the temperature-sensitive CDC25ts Ras guanine nucleotide exchange factor (GEF) mutant [123]. In order to link Ras membrane targeting with PI3K activity, activated Ras (Q61L) [124] is expressed as a fusion protein with the pleckstrin homology (PH) domain of Akt/PKB, and coexpressed with membrane-localized p110β-CAAX [125]. The membrane-localized p110β-CAAX produces PtdIns-3,4,5-P_3, which recruits the PH-Ras fusion protein to the membrane where its activity can complement the loss of CDC25 activity.

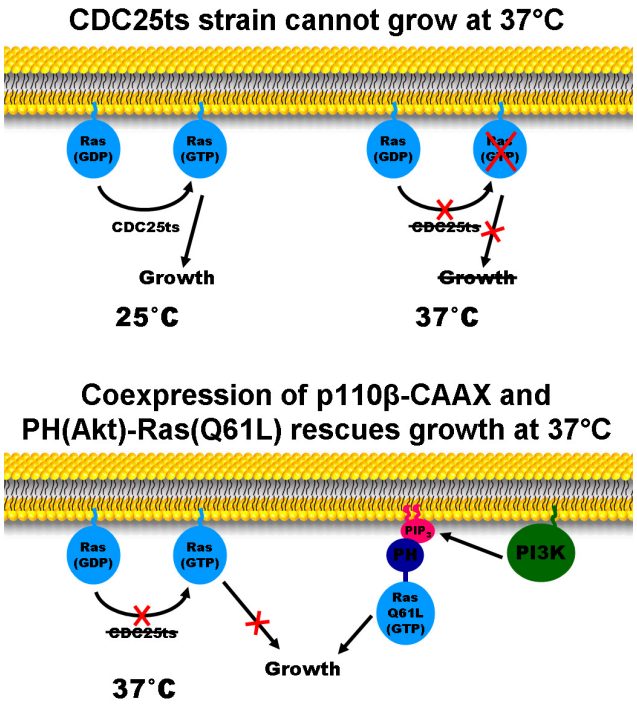

Figure 2.5. S. cerevisiae growth rescue by PI3K activity [125].

2.5.2 Growth rescue by additional p110 isoforms

In addition to replicating the results of previous studies with p110β [125], I introduced the p110α and p110δ isoforms into the PH-Ras PI3K growth rescue system on either high copy (2μ) or low copy (CEN-ARS) plasmids.

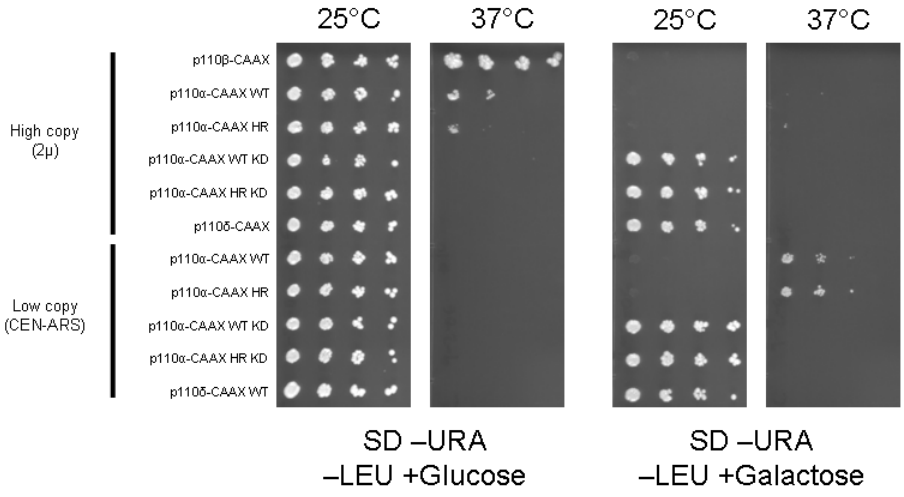

Figure 2.6. Growth rescue by the p110β, p110α, and p110δ isoforms. 1:6 serial dilutions of *CDC25ts* S. cerevisiae expressing PH(Akt)-Ras constitutively and the indicated p110 isoforms under control of the GAL1 promoter. WT = wild type, HR = H1047R mutant, KD = kinase dead mutant.

Interestingly, p110β-CAAX is only able to rescue growth on glucose media, when expression should be completely shut off due to glucose repression of the GAL1 promoter. When grown on galactose media, p110β-CAAX does not rescue growth at the restrictive temperature (37°C), and in fact strongly inhibits growth at the permissive temperature (25°C), indicating that p110β-CAAX is toxic to S. cerevisiae when overexpressed, and only rescues to *CDC25ts* phenotype when expressed at exceedingly low levels. Similar results are seen with p110α-CAAX wild type and H1047R on the high copy vector (2μ), but when expressed on the low copy vector (CEN-ARS), there is no growth rescue on glucose, but moderate growth rescue on galactose. However, with

the p110α vectors there is also strong growth inhibition at the permissive temperature (25°C). p110δ has no detectable kinase activity in this system, because it behaves identically to the kinase dead p110α mutants, showing no growth inhibition at permissive temperatures or growth rescue at restrictive temperatures.

This result suggests that there is a narrow window of PI3K activity that is able to rescue growth in the *CDC25ts* PH-Ras system. If there is too much PI3K activity then the depletion of PtdIns-4,5-P_2 and other phosphoinositides will inhibit yeast growth, but if the PI3K activity is too low then not enough PtsIns-3,4,5-P_3 will be generated to recruit PH(Akt)-Ras(Q61L) to the membrane to compensate for loss of CDC25 activity. Based on the results in Fig. 2.6 it appears the order of activity levels for the different p110 isoform constructs are as follows: p110α kinase dead mutants = high and low copy p110δ < high copy uninduced (repressed) p110β < uninduced (repressed) p110α < high copy induced p110β < low copy induced p110α < high copy induced p110α. The optimal level of PI3K activity to achieve growth rescue appears to be closest to the level of uninduced p110β, which appears to be quite low.

2.5.3 PI3K inhibitors do not inhibit growth rescue by p110β-CAAX

In order to use the PH-Ras growth rescue system as a positive screen for drug-resistant mutations, it must be sensitive enough to monitor PI3K inhibition. Because uninduced (repressed) p110β-CAAX on glucose-containing media at 25°C produces the most robust growth rescue, I performed halo assays with two PI3K inhibitors that target p110β, PI-103 and PIK-108 [20].

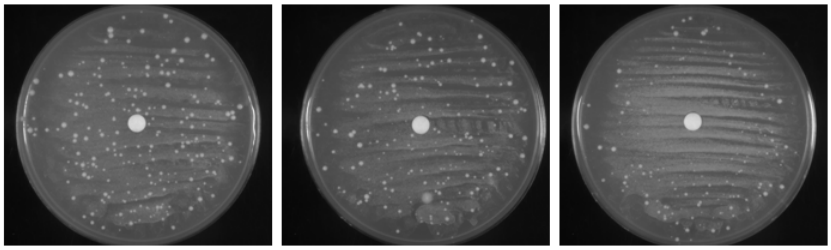

Figure 2.7. CDC25ts PH-Ras PI3K halo assays. The CDC25ts PH(Akt)-Ras(Q61L) p110β-CAAX strain was grown on SD –URA –LEU +Glucose plates at 37°C. 10 µl of a 10 mM stock of each inhibitor was spotted onto a cellulose disc on the center of the plate.

The faint lawn and presence of revertant colonies on the DMSO control plate indicates that growth rescue by p110β-CAAX, while stronger than observed with the p110α and p110δ constructs (Fig. 2.6), is still very weak. This could be due to one of two reasons: if PI3K activity is too low then not enough PtdIns-3,4,5-P_3 is generated to recruit PH-Ras to the membrane, but if PI3K is to high, then the toxicity of depleting PtdIns-4,5-P_2 and other phosphoinositides will override any positive growth effects of PH-Ras membrane recruitment. The result with the two PI3K inhibitors clearly demonstrates that growth rescue is weak due to the second reason: PI3K activity is too high and therefore toxic to the yeast strain. This is because when the lower potency p110β inhibitor PI-103 is used (IC_{50} = 88 nM in vitro at 100µM ATP [20]), the lawn becomes slightly less faint than with DMSO alone, and the revertant colonies decrease near the center of the plate, and when the higher potency p110β inhibitor PIK-108 is used (IC_{50} = 57 nM in vitro at 100µM ATP [20]), the lawn becomes even stronger and the revertant colonies decrease further. Because PI3K inhibition improves growth rather than inhibits it and no halo is observed, it is clear that PI3K activity is greater than ideal for growth in this system.

2.5.4 Modulation of PH-Ras system by introduction of PTEN, p85α, and multiple p110 isoforms

In an attempt to decrease the PI3K activity in the PH-Ras system so it would be usable to study PI3K inhibition and to perform a positive selection for PI3K inhibitor resistance mutations, I introduced p85α and PTEN into the yeast strains. As the phosphatase that opposes PI3K activity by converting PtdIns-3,4,5-P_3 back to PtdIns-4,5-P_2, PTEN is an obvious choice to reduce buildup of PtdIns-3-4-5-P_3 and depletion of other phosphoinositide species. Although p85α stabilizes the p110 isoforms, it also inhibits the PI3K catalytic activity through a negative regulatory interaction [126], so this may also reduce the amount of PI3K activity present in the cell to a less toxic level. In order to increase the chance of finding the ideal PI3K activity level, I introduced PTEN and p85α on plasmids under the control of four different constitutive promoters, rather than the inducible GAL1 promoter used for the p110 isoforms. The relative order of expression level for the four promoters is as follows: CYC1 < ADH < TEF < GPD [127].

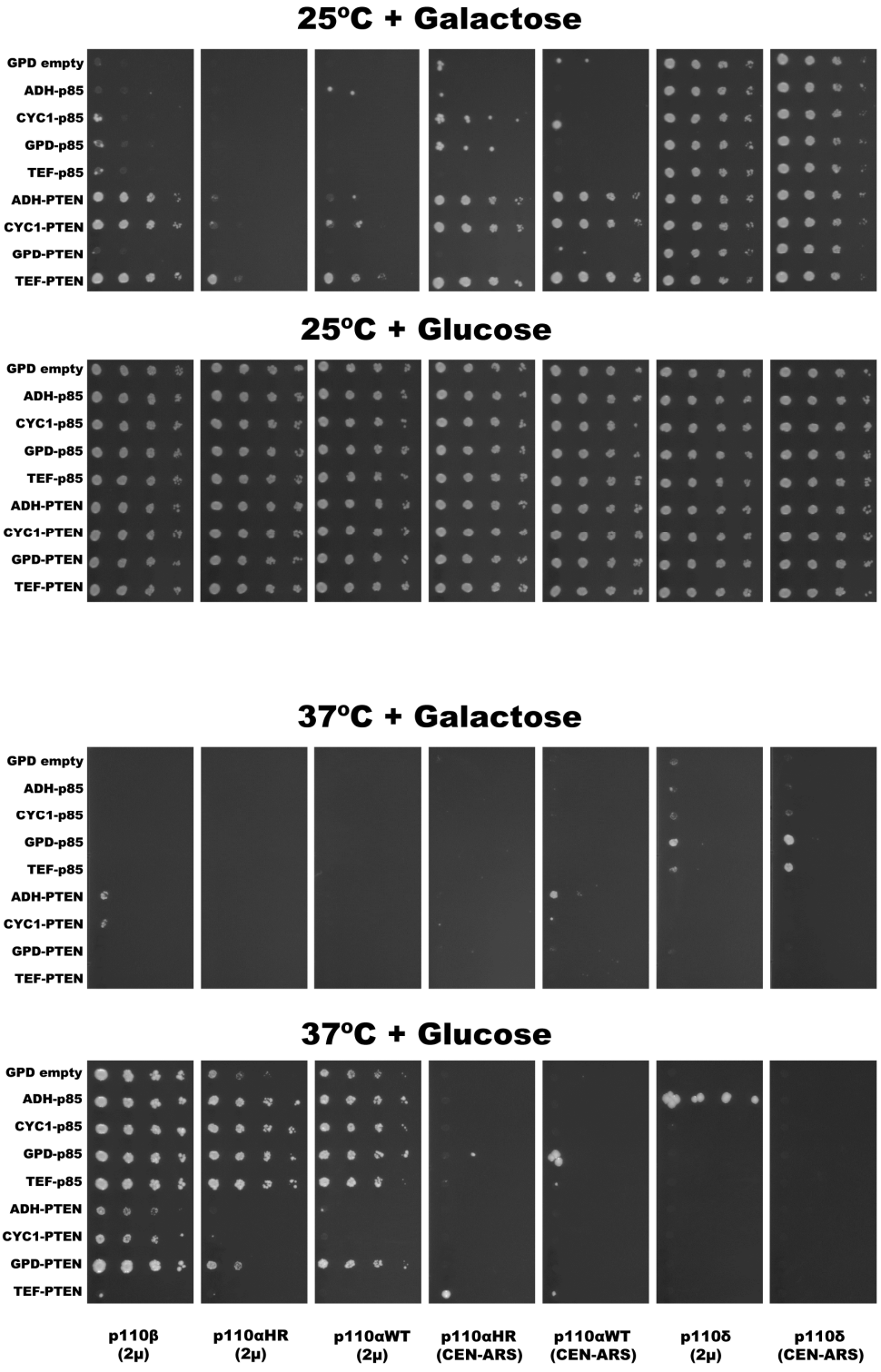

Figure 2.8. Introduction of PTEN and p85α into the CDC25ts PH-Ras PI3K growth rescue system. All p110 isoforms are expressed with a C-terminal CAAX motif. Empty = empty vector, 2μ = high copy, CEN-ARS = low copy, HR = H1047R.

Comparing the galactose plates to the glucose plates at 25°C reveals PI3K-induced toxicity: All PTEN constructs except GPD rescue PI3K-induced toxicity, not surprisingly more so for the low copy than the high copy p110α vectors. The GPD result is surprising and the vector is likely to be non-functional, but this was not investigated further. p85α coexpression does not appear to have a large effect on PI3K-induced toxicity, although the CYC1 and GPD p85α vectors provide a relatively small growth rescue for the low copy p110αWT vector, indicating that p85α coexpression is able to decrease p110α activity very slightly in S. cerevisiae. The galactose plates grown at 37°C suggest that p85α coexpression brings p110δ's PI3K activity to a level that can produce PtdIns-3,4,5-P_3 without excess toxicity. On the glucose plates grown at 37°C, no PTEN or p85α construct is able to complement the CDC25ts phenotype and rescue growth better than the empty vector control with p110β-CAAX.

2.6 Materials and Methods

2.6.1 Yeast strains

The S. cerevisiae strains YRP1 (*Δerg6, Δpdr5, Δsnq2*) and AFS92 were used for all experiments. Strains were grown at 30°C on synthetic dropout (SD) media -Uracil +Glucose or +Galactose. PI3K inhibitors were added to media in DMSO at 1:100.

2.6.2 Yeast plasmids

A C-terminal myristoylation sequence (CAAX box) was added to human p110α-H1047R by three rounds of PCR amplification with the following primers: 1) hp110α-

FM and hp110α-CRM, 2) hp110α-FL and hp110α-CRL. The resulting fragment was cloned into a high copy (2μ), *URA3* yeast expression vector with a *GAL1* promoter by gap repair/homologous recombination to create the vector p*URA3*-2μ-*GAL1*-p110αH1047R-CAAX. Wild-type and kinase-dead plasmids were created by site-directed mutagenesis with the following primers: hp110αR1047H-F, hp110αR1047H-R, hp110αK802R-F, and hp110αK802R-R.

Primer Name	Primer Sequence (5'-3')
hp110α-FM	cctctatactttaacgtcaaggagaaatgcctccacgaccatcatcaggtgaactg
hp110α-CRM	gcgcgcctcatcaagagagcacacacttacagttcaatgcatgctgtttaattgtgtgg
hp110α-FL	gtatcaacaaaaaattgttaatatacctctatactttaacgtcaagg
hp110α-CRL	cgcgtaatacgactcactatagggcgaattgggtaccccggcgcgcctcatcaagagagc
hp110αR1047H-F	aatgatgcacATcatggtggctggacaacaaaaatgg
hp110αR1047H-R	ccagccaccatgATgtgcatcattcatttgtttc
hp110αK802R-F	gagatcatctttCGaaatggggatgatttacggc
hp110αK802R-R	ccccatttCGaaagatgatctcattgttctgaaacagtaactc

Table 2.1. Oligonucleotide primers used for subcloning p110α and site-directed mutagenesis.

2.6.3 Yeast transformation

The AFS92 strain was transformed with plasmid DNA by a standard lithium acetate protocol. This same protocol gave extremely low yields with the YRP1 strain, so an alternative electroporation protocol was used for YRP1, adapted from D. Gottschling, Fred Hutchinson Cancer Research Center, Seattle, WA: http://www.fhcrc.org/science/labs/gottschling/yeast/ytrans.html. Briefly, YRP1 were grown in 50 ml YPD medium at 30°C until early stationary phase (OD_{660} = 1.05-1.25)

and then harvested by centrifugation at 3000 RPM, 4°C, for 5 minutes. The cells were then washed twice with ice-cold sterile distilled H_20, centrifuging at 2500 RPM, 4°C, for 5 minutes, and washed once with ice-cold 1 M Sorbitol, centrifuging at 2000 RPM, 4°C, for 5 minutes. The cells were then resuspended with 1.5 ml ice-cold 1 M Sorbitol, and 80 µl of the cell suspension was mixed with 2 µl plasmid DNA prep (0.5-2 µg) and transferred to a pre-chilled 0.1 cm gap electroporation cuvette (BioRad Genepulser), and electroporated with the following settings: 1.5 kV Voltage, 25 µF Capacitance, 200 Ω Resistance. Immediately after electroporation, the cells were suspended in 1 ml ice-cold 1 M Sorbitol and transferred to a pre-chilled 1.5 ml eppendorf tube, before spreading onto selective media. Transformation efficiencies of 10^5 colonies/µg DNA were routinely observed, greatly improving on the 10^2 colonies/µg DNA efficiency observed with standard Lithium Acetate transformation.

2.6.4 Reverse Halo Assay

Log phase YRP1-p*URA3*-2µ-*GAL1*-p110αH1047R-CAAX cultures grown in SD -Uracil +Glucose were washed three times with water and then spread into a lawn on SD -Uracil +Galactose agarose plates at approximately 10^6 cells per plate. After drying, a small cellulose disc was placed in the middle of each plate, and then 10 µl of a DMSO inhibitor stock was spotted onto the cellulose disc. The plates were incubated at 30°C for 5-7 days before imaging.

2.6.5 PI3K inhibitors

All other inhibitors used in this study were synthesized following previously reported protocols [20, 85, 86]. In all agar plates, DMSO inhibitor stocks were used at 1:100.

2.7 Conclusion

Toward the goal of performing a PI3K inhibitor resistance screen in S. cerevisiae, I developed a sensitive and robust assay to measure p110α inhibition by rescue of PI3K-induced toxicity, and then validated the assay with several small molecule p110α inhibitors by reverse halo assay. PI3K-induced toxicity was used to explore the possibility of drug-resistance mutations at the gatekeeper position of p110α, but this position proved intolerant to mutation. An alternative approach to assaying PI3K inhibition in S. cerevisiae was explored that uses PI3K-induced rescue of growth rather than PI3K-induced toxicity, but the inherent toxicity of PI3K activity in S. cerevisiae made this strategy not viable.

3 A mutagenic screen in S. cerevisiae for PI3K inhibitor resistance

3.1 Introduction

To determine whether p110α is susceptible to drug-resistant mutations in a similar manner to protein kinases, I mutagenized residues that line the affinity pocket and screened against a structurally diverse panel of PI3K inhibitors. Using a highly parallel approach with robotic pinning, I generated a measure of catalytic activity and an inhibition profile for every clone in our mutant library, allowing for a detailed structure-function analysis of the p110α affinity pocket. In addition to drug-resistant p110α mutations, I was able to identify drug-sensitizing mutations as well due to the large dynamic range of the S. cerevisiae assay and the ability to replicate the same mutant library onto multiple agar plates with varying drug concentrations.

3.2 Library Generation

In section 3.4, the p110α gatekeeper residue Ile 848 appeared relatively intolerant to mutation, so in order to identify potential resistance mutations, I expanded the screen to include more residues. As explained in section 3.5, the PI3K-induced toxicity assay in S. cerevisiae can only be used as a negative screen for drug resistance, which is orders of magnitude lower throughput than a positive selection. Given the relatively low throughput of a negative screen, mutagenizing the full length p110α protein, or even just the kinase domain, was deemed prohibitive. Therefore, a focused screen was adopted, zeroing in on the active site residues most likely to give rise to drug resistance if mutated.

The screen was expanded from the gatekeeper residue Ile 848 to include seven additional residues surrounding the p110α affinity pocket [20].

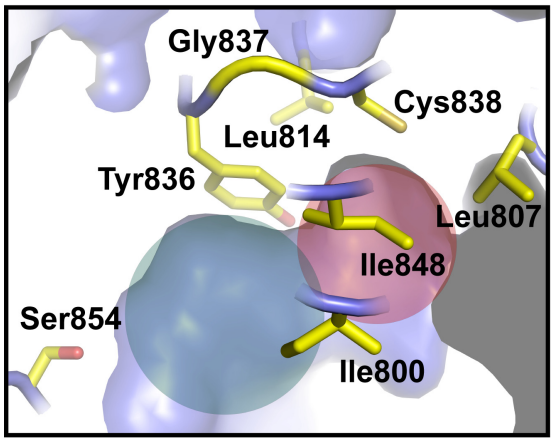

Figure 3.1. Affinity pocket residues chosen for saturation mutagenesis. Residues are shown on the p110α structure (PDB code 2RD0).

These residues were chosen because the affinity pocket is occupied by most potent PI3K inhibitors, but not by ATP [20], making it a likely site for drug-resistant mutations. Ile 800, Leu 807, Leu 814, Tyr 836, Gly 837, Cys 838, and Ile 848 were chosen based on proximity to the affinity pocket, and lack of interaction with the catalytic Lys 802, DFG

motif (responsible for Mg^{2+} coordination), or ATP. One additional residue outside the affinity pocket, Ser 854, was chosen due to possible inhibitor-specific H-bonds. These eight residues are highly conserved in the PI3K family and almost 100% identical among the p110 isoforms.

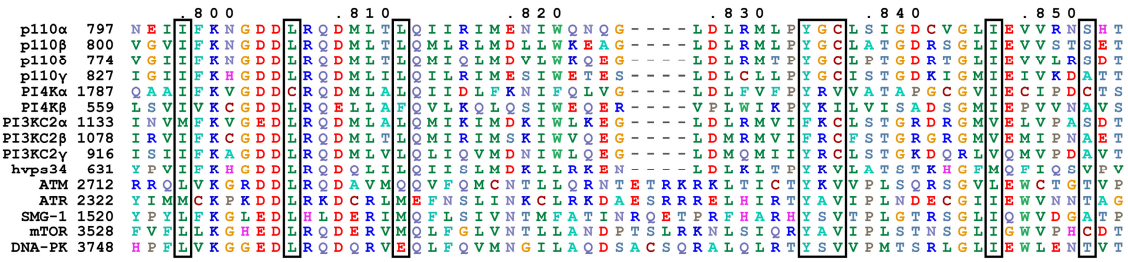

Figure 3.2. Sequence alignment of the human PI3K family. Affinity pocket residues chosen for saturation mutagenesis are indicated by boxes.

3.2.1 NNK mutagenesis and YRP1 transformation

Each chosen residue was subject to saturation mutagenesis with randomized NNK primers, and then each single residue library was transformed in E. coli. The resulting E. coli colonies were pooled into a single pellet from which plasmid prep DNA was isolated for each single residue library.

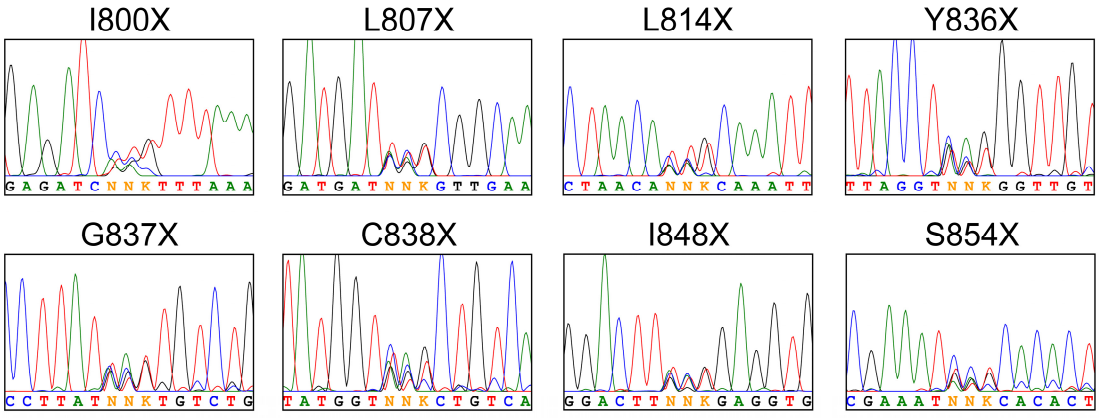

Figure 3.3. DNA sequencing chromatograms of the p110α mutagenic libraries. Randomized codons of the p110α affinity pocket NNK libraries, sequenced with the following primer: (5'-3') ACCCAGATCCTATGGTTCGAGG.

The resulting eight single residue plasmid DNA libraries were transformed into the yeast strain YRP1 using the electroporation protocol from section 3.6.3, producing libraries ranging in size from 1000 – 3000 colonies.

3.3 Robotic 384-pin format library replication and image analysis

384 YRP1 colonies from each NNK library were picked and arrayed onto 384-pin format plates, and then robotically replicated onto glucose and galactose plates to determine the PI3K activity of each clone by colony size, measured with Cellprofiler image analysis software [128].

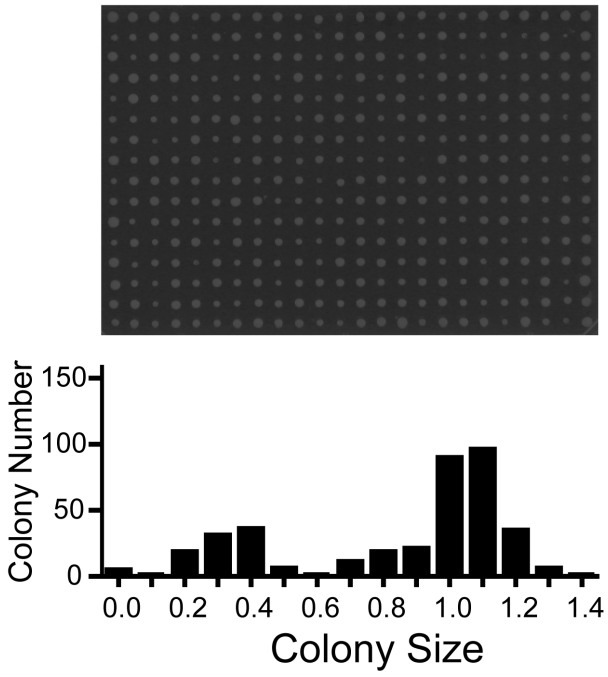

Figure 3.4. Growth inhibition profile of a representative NNK library in the YRP1 strain. The mutant library was pinned onto SD -Uracil +Galactose and grown for 5 days at 30°C, and the distribution of colony sizes for that plate was calculated relative to the same array plated on SD -Uracil +Glucose and grown for 3 days at 30°C (not shown).

3.4 Active site residues' tolerance to mutation

In order to determine how tolerant each p110α affinity pocket residue is to mutation, I compared the colony size distributions generated for each residue in the course of our mutagenic screen.

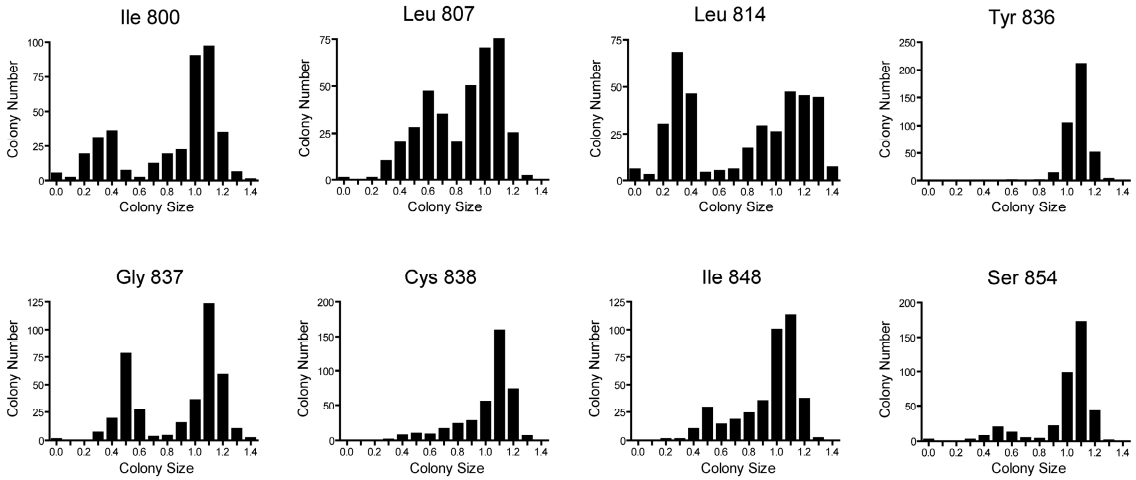

Figure 3.5. Tolerance to mutation in the p110α affinity pocket. Colony size distributions for 384 colony arrays of the indicated p110α mutant libraries, grown in the YRP1 strain on SD -Uracil +Galactose media as described in Fig. 3.4.

All mutant libraries display a peak of relative colony sizes close to 1.0, corresponding to no growth inhibition and therefore kinase-dead mutants. The majority of mutant libraries also display a second peak of smaller colony sizes, corresponding to growth inhibition and therefore PI3K activity. The tolerance to mutation for each residue was quantified by $\Sigma(1-x)^2$, where x equals relative colony size. The resulting values were converted into heat map color scale and displayed on the crystal structure of p110α.

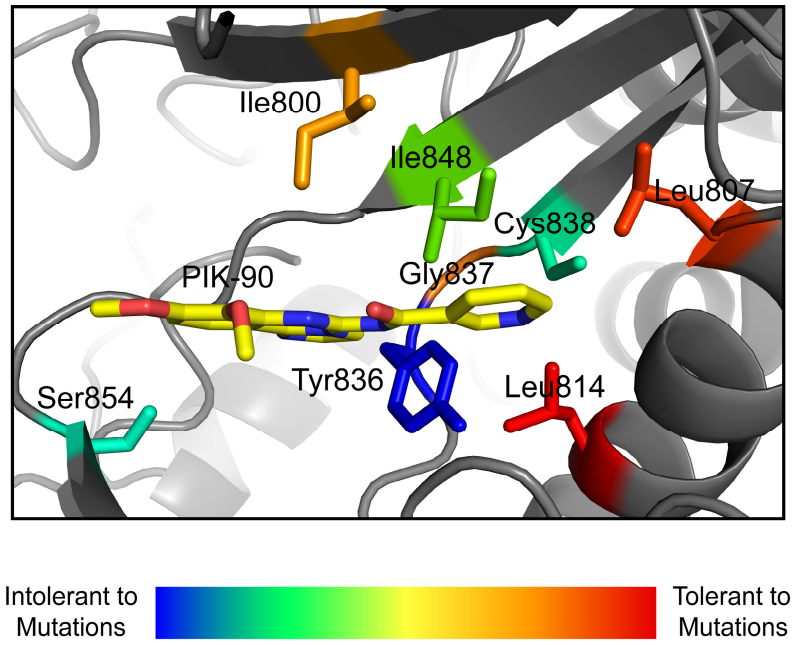

Figure 3.6. Structural representation of tolerance to mutation in the p110α affinity pocket. Mutational tolerance is calculated by $\Sigma(1\text{-}x)^2$ from the distributions in Fig. 3.5, where x equals relative colony size. These values were converted into heat map values and are shown on the p110α crystal structure (PDB code 2RD0) with the PI3K inhibitor PIK-90 from the p110γ co-crystal structure (PDB code 2CHX) overlaid by structural alignment.

The Ile 800, Ile 807, Leu 814, and Gly 837 residues are most tolerant to mutation, Cys 837, Ile 848, and Ser 854 are less tolerant to mutation, and Tyr 836 appears to be completely intolerant to mutation, with even the conservative mutation T836F causing a substantial loss of kinase activity. Intolerance to mutation at Tyr 836 corroborates previous results with p110α [106]. Recently published work has shown that the mutation corresponding to Y836M in PI4KIIIβ produces an active kinase that is resistant to Wortmannin and PIK-93, and the same mutation in PI4KIIIα kills all catalytic activity [129]. It is currently unclear why this mutation is tolerated in PI4KIIIβ but abolishes kinase activity in PI4KIIIα and p110α. Further experiments with additional PI3K family

members may better reveal the sequence determinants for mutation tolerance and inhibitor sensitivity.

3.5 PI3K inhibitor screen

Only active mutants were screened against PI3K inhibitors in order to avoid the unwanted "neighboring" effects of inactive clones: colonies with inactive PI3K grow much faster than the surround active mutants and use up the surrounding nutrients, resulting in smaller than expected colonies in the surrounding grid. Active mutants with relative colony sizes less than 70% of wild-type were picked and arrayed onto new 384-pin format plates, and then these new pooled arrays were replicated onto multiple PI3K inhibitor containing plates to screen for drug resistance and sensitization.

	Low	Medium	High
PIK-85	2 μM	10 μM	20 μM
PIK-93	2 μM	10 μM	20 μM
PI-103	1 μM	2 μM	5 μM
PW-12	100 nM	500 nM	2 μM
PP-110	2 μM	10 μM	not done

Table 3.1. Inhibitor concentrations used in the p110α mutant screen. PIK-85 was used in place of PIK-90 for all screens; it is identical to PIK-90 except for an enol group in place of PIK-90's amide (Fig. 1.9).

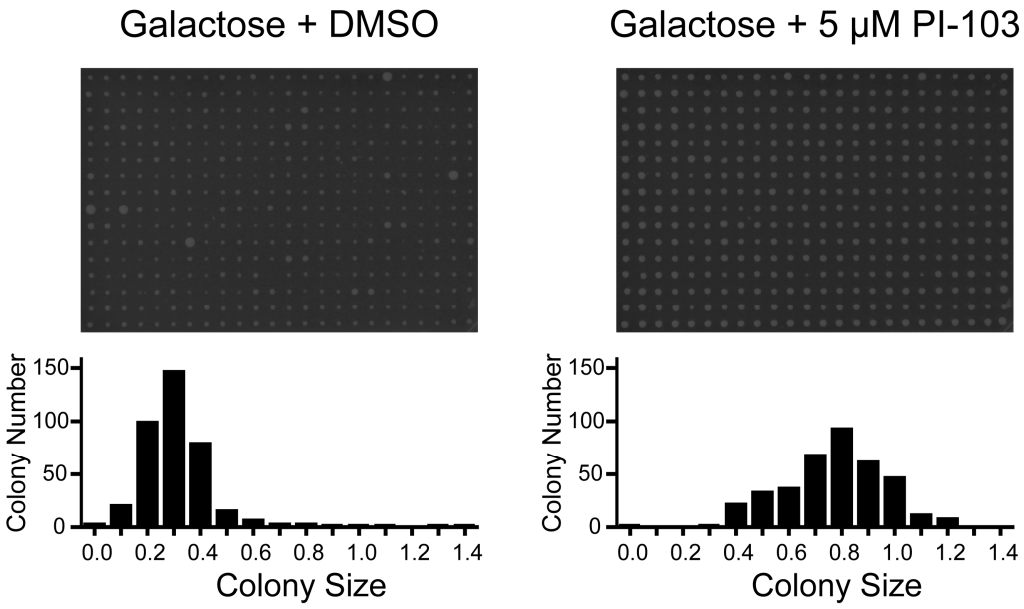

Figure 3.7. Representative images and the corresponding colony size distributions of a pooled active mutant library. The colonies were pinned onto SD -Uracil +Galactose with either DMSO or 5 μM PI-103 and grown for 5 days at 30°C.

3.6 Identification of drug-resistant and drug-sensitized p110α mutations

Drug-resistant p110α mutants were identified by continued growth inhibition at drug concentrations that rescue growth from wild-type p110α. An unexpected benefit of the yeast screen was the ability to identify drug sensitization in addition to drug resistance, by enhanced growth rescue at low inhibitor concentrations that do not rescue growth from wild-type p110α. Currently there is no truly selective p110α inhibitor available, so the drug-sensitized mutants we identified will be valuable tools for the study of p110α's role in biological processes that rely on PI3K signaling, from oncogenesis and tumor maintenance [10, 11] to processes as varied as neuronal development and animal behavior, viral replication, and stem cell self-renewal [130-134].

3.7 Screen hit serial dilution growth assays

Potential drug-resistant and drug-sensitized clones identified on the 384-pin inhibitor plates were validated by serial dilution analysis.

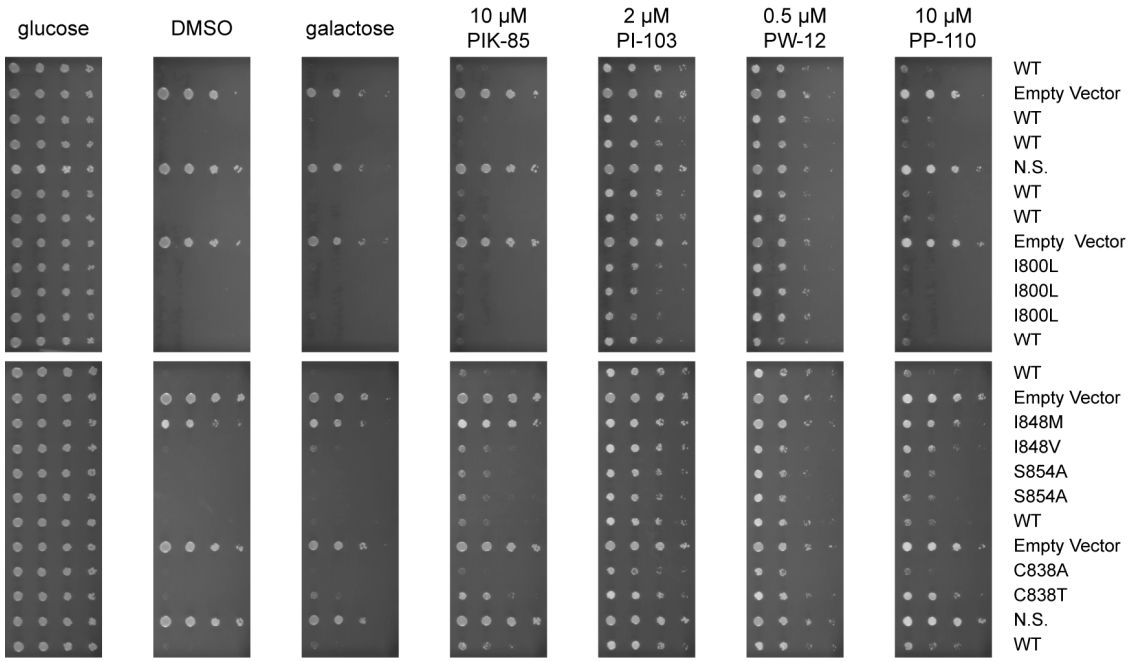

Figure 3.8. Representative plates showing the characterization of yeast screen hits by serial dilution analysis. Six-fold serial dilutions of the screen hit strains were incubated at 30°C for 2 days (glucose) and 6 days (galactose). Strains that were not sequenced are labeled N.S. (not sequenced). Strains that were unable to be sequenced due to plasmid rescue failure are labeled U.S. (unable to sequence).

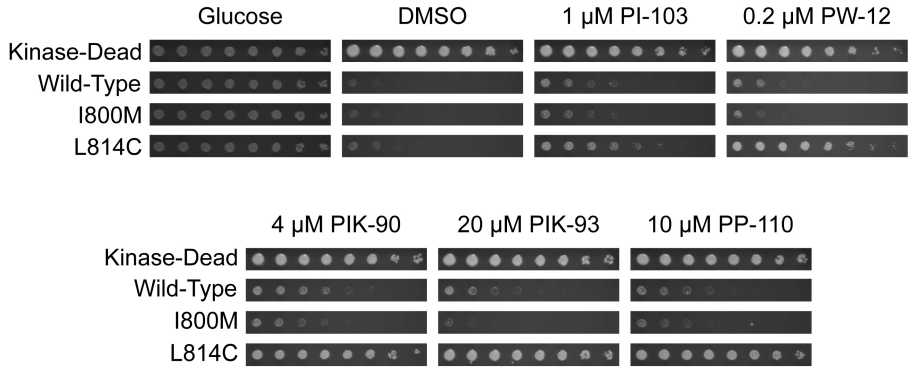

Figure 3.9. 1:3 Serial dilutions of the most promising drug-resistant (I800M) and drug-sensitized (L814C) strains. The growth assay was performed as in Fig. 3.8.

3.8 Materials and Methods

3.8.1 Screen Outline

Residues of interest were subject to saturation mutagenesis with randomized primers, and the resulting libraries were transformed into the permeablized yeast strain YRP1. Individual colonies were picked and arrayed into 384-pin format and then replicated with a robotic pinner onto glucose and galactose-containing media to determine the relative colony size, and therefore PI3K activity, of each mutant clone. Active mutants were picked and arrayed onto new 384-pin format plates and then replicated onto multiple PI3K inhibitor plates to screen for drug resistance and sensitization.

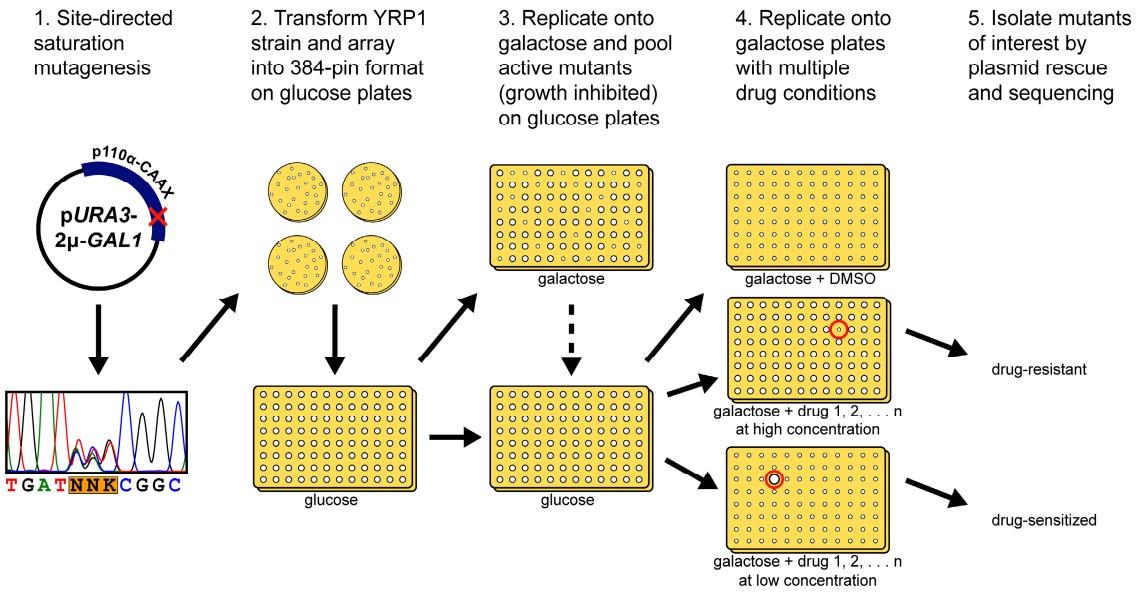

Figure 3.10. S. cerevisiae Screen Outline.

3.8.2 NNK mutagenesis and library creation

The yeast expression vector p*URA3*-2μ-*GAL1*-p110αH1047R-CAAX was mutagenized at the residues Ile 800, Leu 807, Leu 814, Tyr 836, Gly 837, Cys 838, and Ser 854 by quickchange PCR with degenerate NNK primers, where N = 25% A, 25% C, 25% G, 25% T, and K = 50% G, 50% T.

Primer Name	Primer Sequence (5'-3')
I800-Forward	caatgagatcNNKtttaaaaatggggatgatttacggcaagatatgc
I800-Reverse	catttttaaaMNNgatctcattgttctgaaacagtaactctgacatgatgtctgg
L807-Forward	gggatgatNNKcggcaagatatgctaacacttcaaattattcg
L807Reverse	catatcttgccgMNNatcatccccatttttaaagatgatctcattg
L814-Forward	gatatgctaacaNNKcaaattattcgtattatggaaaatatctggc
L814-Reverse	cgaataatttgMNNtgttagcatatcttgccgtaaatcatcccc
Y836-Forward	cgaatgttacctNNKggttgtctgtcaatcggtgactgtgtgggac
Y836-Reverse	ccgattgacagacaaccMNNaggtaacattcgaagatcaagacc
G837-Forward	cgaatgttaccttatNNKtgtctgtcaatcggtgactgtgtgggac
G837-Reverse	ccgattgacagacaMNNataaggtaacattcgaagatcaagacc
C838-Forward	cgaatgttaccttatggtNNKctgtcaatcggtgactgtgtgggac
C838-Reverse	ccgattgacagMNNaccataaggtaacattcgaagatcaagacc
I848-Forward	tgtgggacttNNKgaggtggtgcgaaattctcacactattatgc
I848-Reverse	gcaccacctcMNNaagtcccacacagtcaccgattgacagac
S854-Forward	gtgcgaaatNNKcacactattatgcaaattcagtgcaaaggcggc
S854-Reverse	gcataatagtgtgMNNatttcgcaccacctcaataagtccc

Table 3.2. Primers used for saturation mutagenesis.

The resulting PCR reactions were purified with a Qiagen PCR Cleanup kit, DpnI digested for 90 minutes, and then re-purified. 5 μl of each purified, digested PCR product was transformed into TOP-10 One Shot chemically competent *E. coli* (Invitrogen) and plated

onto a single 10 cm plate of LB media with carbenicillin antibiotic, yielding 1-4 x 10^3 colonies per transformation. Colonies were grown for 2 days at 37°C and then pooled by scraping, transferred to 1.5ml tubes, and spun down to pellets of approximately 0.5 ml. Plasmid DNA was isolated from each pellet with the Qiagen Miniprep kit and verified by restriction digest and DNA sequencing.

3.8.3 YRP1 transformation, robotic pinning, drug screen, and image analysis

p110α NNK libraries were transformed into YRP1 by electroporation and plated onto SD -Uracil +Glucose media. 384 colonies from each library were arrayed by hand and then replicated with a Virtek colony arrayer (Waterloo, Ontario, Canada) to obtain uniformly sized colonies. The arrays were further replicated onto two media conditions: 1) SD -Uracil +Galactose media with added PI3K inhibitor or DMSO alone, and 2) SD -Uracil +Glucose media. The plates were incubated at 30°C until the colonies had grown sufficiently (2-7 days depending on strain and media conditions) and then photographed. Colony size was calculated with Cellprofiler image analysis software, available at www.cellprofiler.org, and each SD -Uracil +Galactose colony size value was divided by the corresponding SD -Uracil +Glucose colony size to normalize for variation in pinning efficiency.

3.8.4 Structural Analysis

Visualization and structural alignment of x-ray crystal structures was performed with the Pymol Molecular Graphics System, available at http://www.pymol.org.

3.9 Conclusion

In this chapter, I describe a resistance screen based on PI3K-induced growth inhibition of S. cerevisiae. Unlike resistance screens based on oncogenic transformation of mammalian cells, this screen allows for the identification of drug-sensitized mutants in addition to drug-resistant mutants, and allows for detailed structure-function analysis of the drug target, because activity levels and inhibitor sensitivities are determined for every clone in the mutant library. Previous studies have used growth inhibition in S. cerevisiae by heterologous expression of a mammalian drug target to screen a compound library for potent inhibitors [135], but to my knowledge such a screen has never been used to identify drug-resistant and drug-sensitizing mutations in the target protein. In addition to p110α, several other drug targets inhibit S. cerevisiae growth, including Akt/PKB, PDK1, p38 kinase, Src, RhoA, RhoC, PARP-1, and HIV Protease [113, 136], and the methods described here should be broadly applicable for the identification of drug-resistant and drug-sensitizing mutations in these proteins as well.

My results in S. cerevisiae indicate that the p110α gatekeeper residue Ile 848 will not be a hotspot for inhibitor resistance in p110α as it is in the protein kinase family. While protein kinases can tolerate dramatic mutations at the gatekeeper position, from smaller, space-creating mutations that sensitize protein kinases to analog-specific inhibitors [96], or larger, steric clash-inducing mutations that confer inhibitor resistance [104], it appears that p110α cannot tolerate significant mutations at this position. This suggests the possibility that the PI3K fold is less tolerant of mutations than the protein kinase fold in this region, which may reduce the clinical development of resistance to p110α-targeted

drugs, although a more complete mutagenic screen of p110α would be required to prove this conclusively.

4 Extension of yeast screen hits

4.1 Introduction

Drug-resistant and drug-sensitizing mutations identified by the yeast screen require validation in a mammalian context, to confirm that their altered activities and inhibitor sensitivities are not due to membrane localization by the C-terminal CAAX box motif, lack of a p85 binding partner, or other artifacts of S. cerevisiae expression. Potential drug-resistant and drug-sensitizing mutations identified with the yeast screen were further characterized in mammalian systems to rule out artifacts from heterologous yeast expression: by kinase assays following expression in the human cell line HEK-293T, and by transformation assays with the human breast epithelial cell line MCF10A.

4.2 In vitro kinase assays

Mutations of interest were introduced into Myc-tagged p110α-H1047R, and then expressed in the human cell line HEK-293T for purification and enzymatic assay.

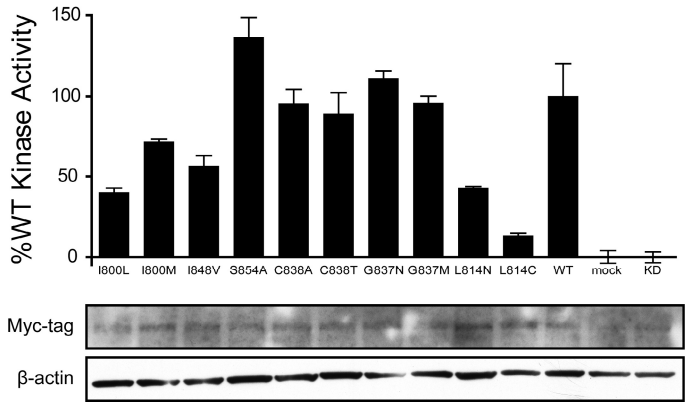

Figure 4.1. Kinase activity of p110α screen hit mutants. The indicated Myc-tagged p110αH1047R mutants were immunoprecipitated from HEK-293T cells and assayed for PI3K activity. Data are represented as mean ± SEM.

Most of the mutants tested have slightly reduced activity: I800L and I800M show approximately 2-fold decreases in PI3K activity, while L814C's activity is significantly reduced. In vitro IC_{50} values were determined for all p110α mutants against the inhibitors used in the yeast screen, as well as BEZ-235, which I obtained after the PI3K inhibitor resistance screen in S. cerevisiae was performed.

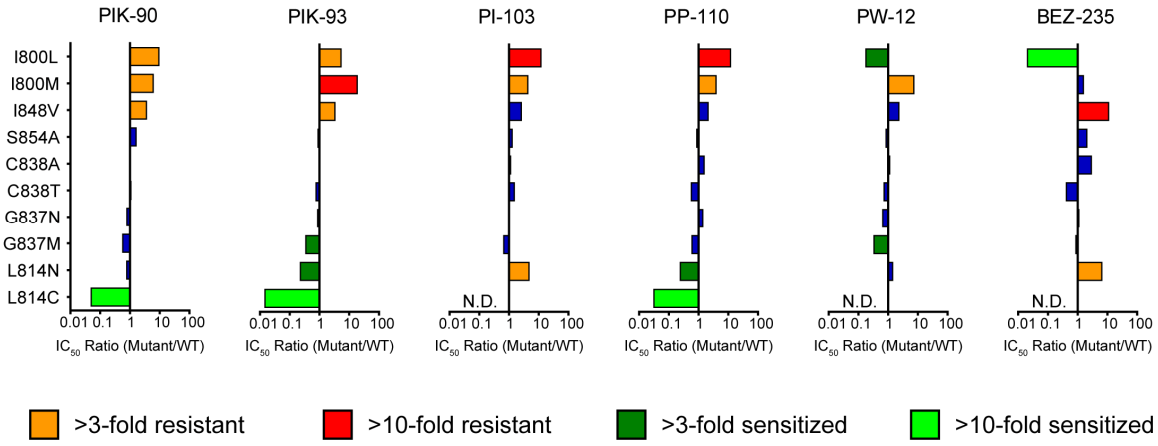

Figure 4.2. Altered inhibitor sensitivities of the p110α screen hit mutants. In vitro IC_{50} values were determined at 10 μM ATP. Changes in inhibitor sensitivity are shown as the ratio of mutant IC_{50} / WT IC_{50}. The label N.D. (not determined) indicates that the data from the performed dose response experiment were insufficient to generate an IC_{50} curve.

Mutation at Ile 800 confers the greatest drug resistance, with both I800L and I800M showing approximately 5-10 fold decreases in inhibitor potency for PIK-90, PIK-93, PI-103, and PP-110, although I800L is sensitized to the compounds PW-12 and BEZ-235. Mutation at Leu 814 confers the greatest drug sensitization, with the L814C mutant sensitized more than 10-fold to PIK-90 and PP-110, and approximately 100-fold to PIK-93.

4.3 MCF10A transformation

The oncogenic potentials of the most drug-resistant and drug-sensitized p110α mutants were assessed in the untransformed breast cell line MCF10A, which requires Epidermal Growth Factor (EGF) for growth under normal tissue culture conditions, but can be transformed to EGF-independent growth by p110α-H1047R [53]. I800L, I800M, L814C, wild-type, and kinase-dead (K802R) mutations were made in the retroviral plasmid pMIG-p110α-H1047R, and then transduced into MCF10A cells. The pMIG vector contains an internal ribosome entry site (IRES)-GFP sequence: infected MCF10A cell lines were all FACS sorted to greater than 95% GFP positive for use in further experiments. In all p110α-transduced MCF10A cell lines, GFP signal was 1-2 orders of magnitude below that of the empty vector control, although still well above background levels.

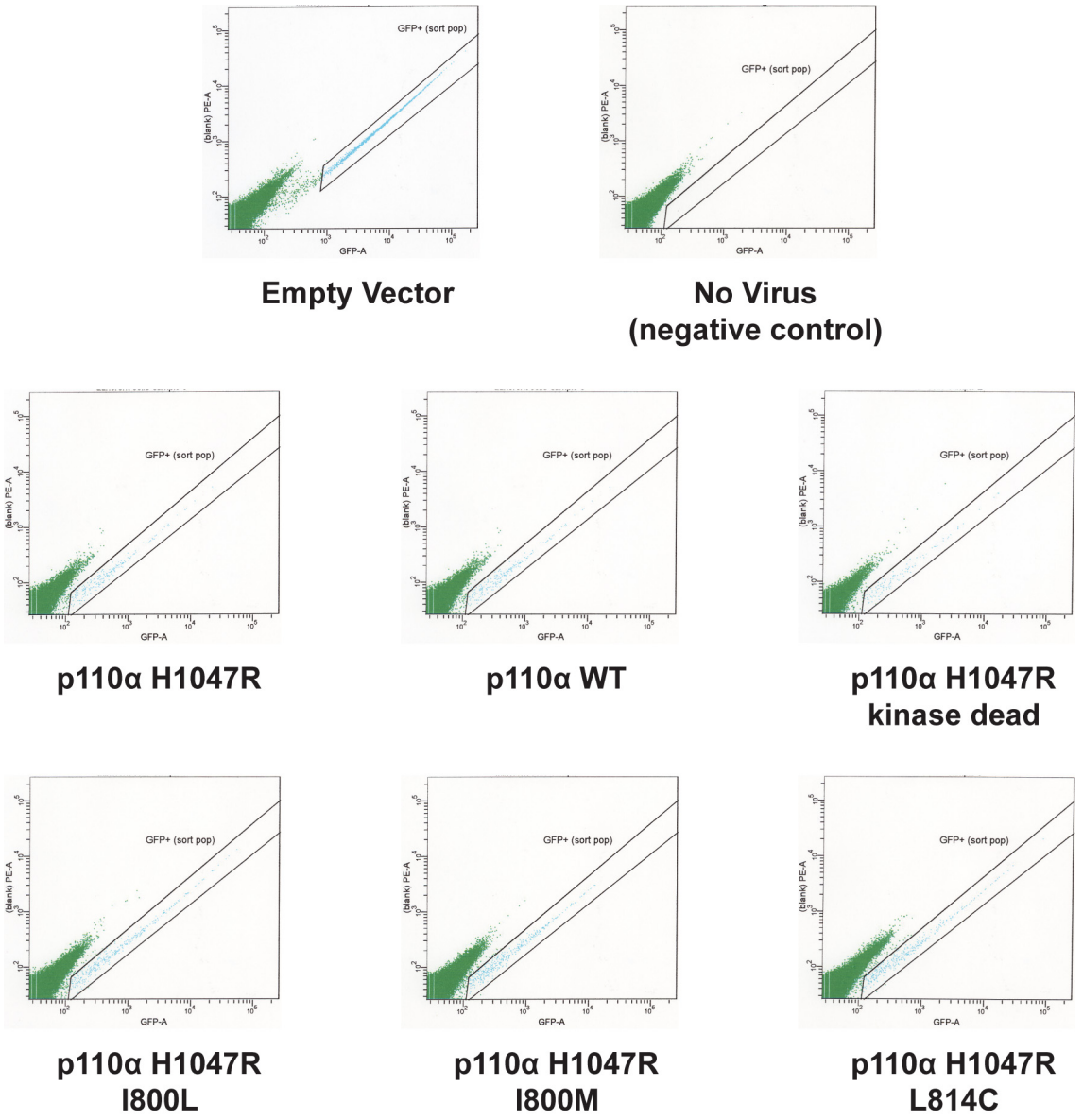

Figure 4.3. GFP signal relative to side scatter observed during MCF10A FACS sorting.

p110α-expressing MCF10A cell lines were cultured in media without EGF to determine whether the drug-resistant and drug-sensitized mutant p110α-H1047Rs could support EGF-independent growth. The I800L and I800M mutant cell lines grow at the same rate as p110α-H1047R, while the L814C mutation caused a small but consistent decrease in growth.

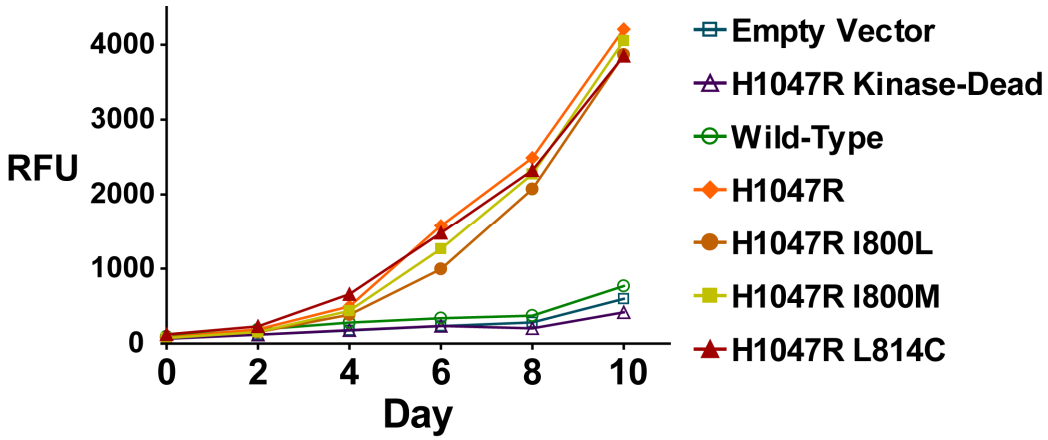

Figure 4.4. EGF-independent growth of MCF10A cell lines expressing oncogenic p110α with drug resistant or sensitizing mutations. Relative Fluorescence Units (RFU) approximates cellular growth, as resazurin added to the media is reduced to the fluorescent species resorufin by metabolically active cells [137, 138].

As all three MCF10A cell lines expressing resistant or sensitized p110α mutants behaved similarly to p110α-H1047R expressing cell line, they were then cultured in the presence of PI3K inhibitors, to determine whether the mutants' changes in inhibitor sensitivity observed in S. cerevisiae and in vitro kinase assays were maintained in vivo during oncogenic transformation.

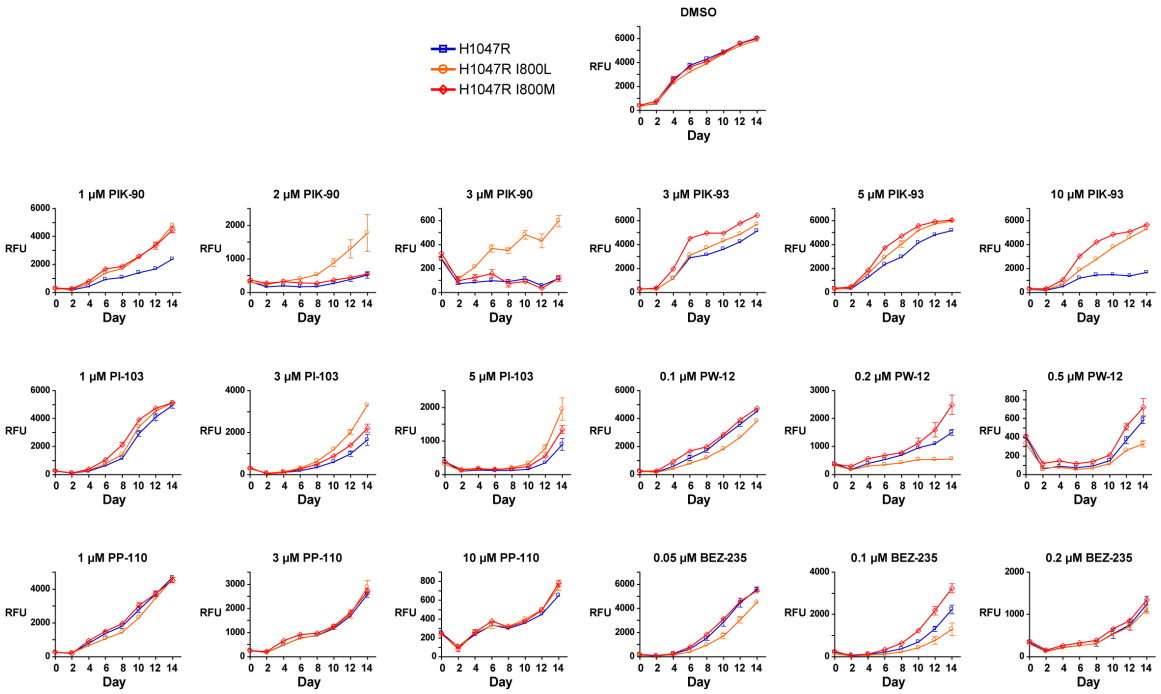

Figure 4.5. Altered in vivo inhibitor sensitivities of the resistance mutants I800L and I800M. Growth in media lacking EGF was monitored as in Fig. 4.4 in the presence of PI3K inhibitors at the indicated concentrations.

I800L and I800M confer resistance to all inhibitors, with the exception that I800L is sensitized to PW-12 and BEZ-235, as seen in the in vitro kinase assays. PI3K inhibitor resistance is most pronounced with the selective PI3K inhibitors PIK-90 and PIK-93, and less dramatic against the multi-targeted PI3K inhibitors PI-103 and BEZ-235 (mTOR), PW-12 (multiple protein kinases), and PP-110 (receptor tyrosine kinases) [20, 83-86, 139, 140].

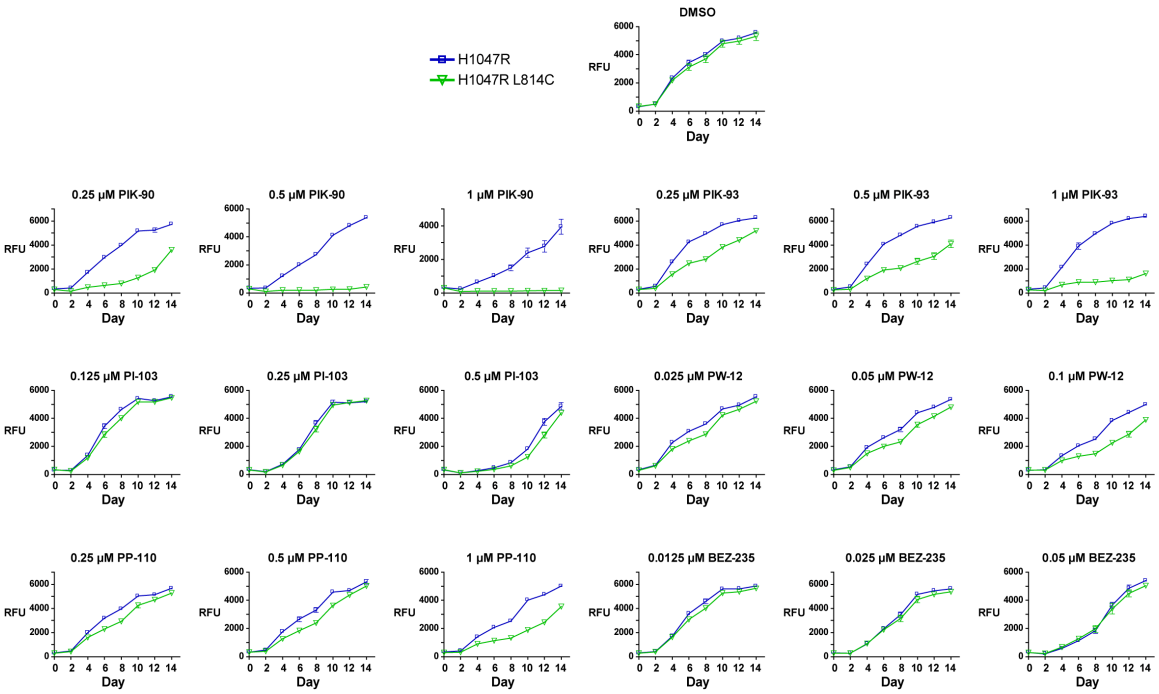

Figure 4.6. Altered in vivo inhibitor sensitivities of the drug-sensitized mutant L814C. Growth in media lacking EGF was monitored as in Fig. 4.4 in the presence of the indicated PI3K inhibitors.

L814C confers strong sensitization of cell growth to PIK-90 and PIK-93, moderate sensitization to PW-12 and PP-110, and minimal or no sensitization to PI-103 and BEZ-235, again likely due to the selectivity of PIK-90 and PIK-93, and the relative promiscuity of PW-12, PP-110, PI-103, and BEZ-235.

Phosphorylation of Akt/PKB residues T308 and S473 was monitored in the I800L, I800M, and L814C-expressing MCF10A cell lines to determine whether these p110α mutants retain the ability to activate the canonical downstream PI3K signaling pathway.

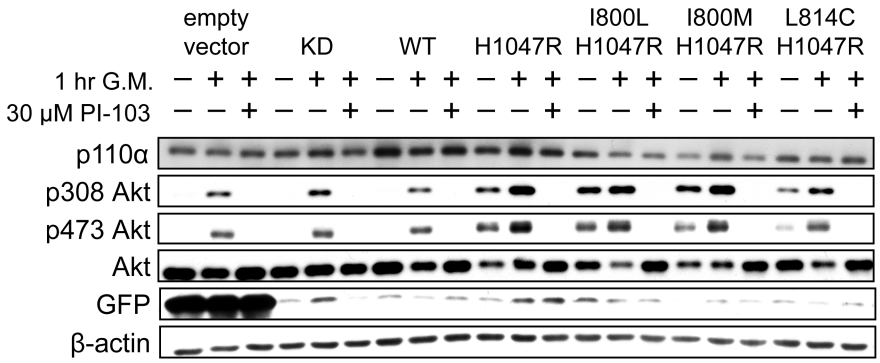

Figure 4.7. Akt/PKB signaling downstream of drug-resistant and drug-sensitized p110α mutants. MCF10A cell lines expressing the indicated p110α mutants were cultured in growth media lacking EGF for 24 hours, and then treated with the indicated combinations of normal growth media (G. M.) and 30 μM PI-103. After 1 hour, the cells were lysed and subject to western blot analysis with the indicated antibodies.

The I800L and I800M mutations to p110αH1047R produce high phospho-Akt levels comparable to p110αH1047R after 24 hours EGF starvation, but L814C gives reduced, although still detectable levels. Phospho-Akt can be fully recovered in all cell lines by one hour treatment with EGF-containing media, and this stimulation can be blocked in all lines by 30 μM PI-103. GFP levels, which are coupled to p110α expression by an IRES promoter, are greatly reduced in all p110α-expressing cell lines, and p110α levels are not highly elevated in comparison to the empty vector control. This is similar to what was observed during the FACS GFP sort (Fig. 4.3) and suggests that MCF10A cells cannot tolerate overexpression of p110α-H1047R. Expression of p110αH1047R or the drug-resistant/sensitized mutants near endogenous levels is sufficient for Akt activation and transformation to EGF independence.

The I800L, I800M, and L814C cell lines were treated with PI3K inhibitors in serial dilution to determine how each mutation affects the inhibitor sensitivity of phospho-Akt levels.

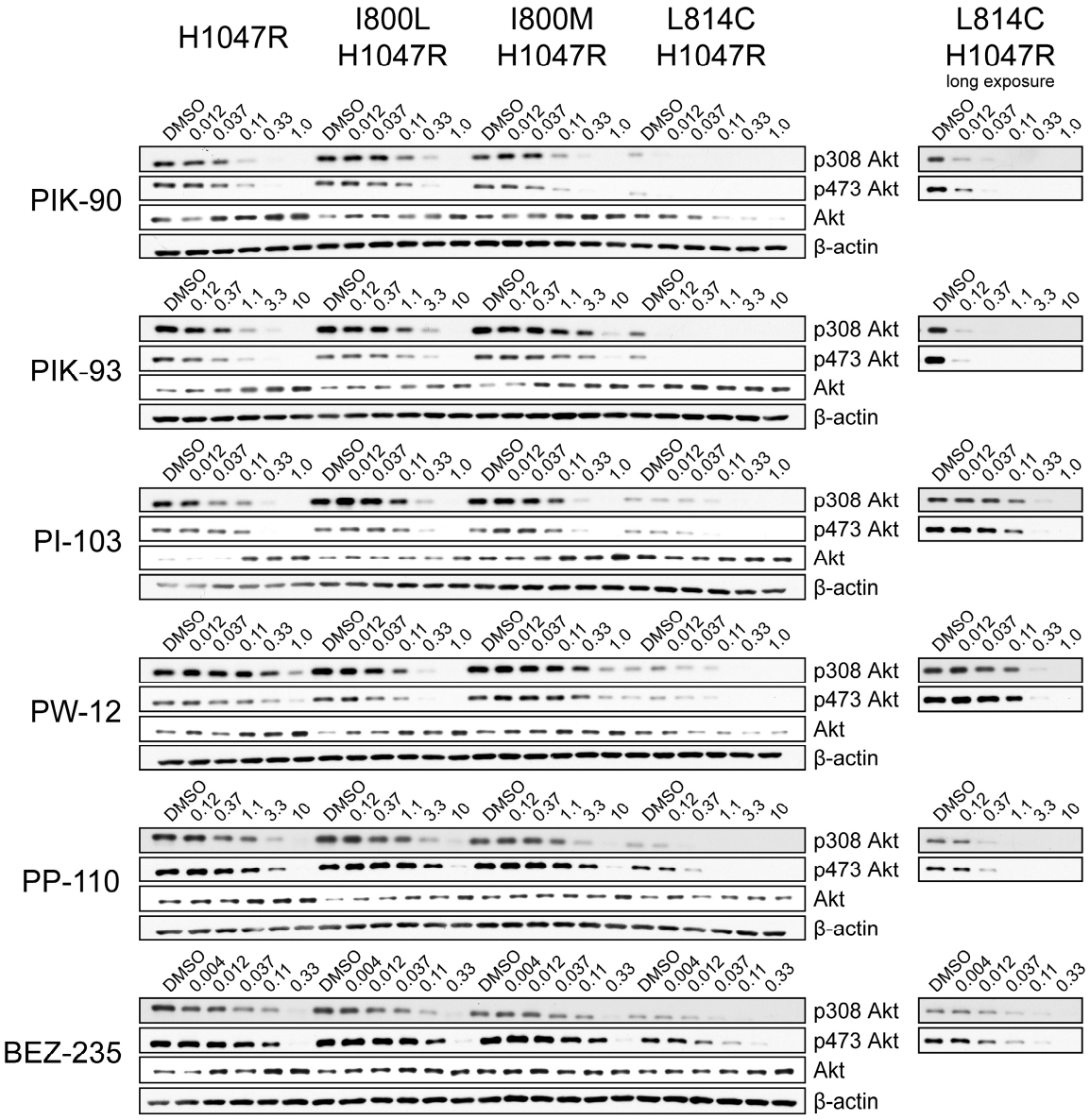

Figure 4.8. Akt/PKB signaling in response to PI3K inhibitors. The indicated MCF10A cell lines were cultured in growth media lacking EGF for 24 hours, and then treated for 1 hour with serial dilutions of the indicated PI3K inhibitors, after which the cells were lysed and subjected to western blot analysis with the indicated antibodies. The PI3K inhibitor concentrations are indicated in μM.

Similar to the MCF10A growth curves, the most striking resistance and sensitization occurs with the selective PI3K inhibitors PIK-90 and PIK-93, most likely because these results are not confounded by off-target effects. I800L is approximately 3-fold resistant

to PIK-90 and PIK-93, I800M is approximately 10-fold resistant to PIK-93, and L814C is approximately 5-fold and 30-fold sensitized to PIK-90 and PIK-93 respectively, consistent with in vitro kinase assays and the MCF10A growth curves. Significant resistance is not observed against the multi-targeted inhibitors PI-103, PW-12, PP-110 and BEZ-235, but sensitization is seen with I800L to PW-12 and L814C to PW-12, PP-110, and BEZ-235, again consistent with in vitro kinase assays and the MCF10A growth curves. Slight resistance and sensitization are observed with the I800L mutant to the dual PI3K/mTOR inhibitors PI-103 and BEZ-235 respectively. This trend is seen in phospho-T308 Akt but not phospho-S473, most likely because mTOR is the kinase that phosphorylates Ser 473 in these cells [141].

4.4 Materials and Methods

4.4.1 Plasmids

Mammalian Expression Plasmids: An N-terminal Myc tag was added to human p110α-H1047R by PCR with the following primers: p110α-BamHI-NtermMyc-F and p110α-EcoRV-R. The resulting fragment was digested with BamHI and EcoRV, and then ligated into the mammalian expression vector pcDNA3 to create pcDNA3-Myc-p110α-H1047R. Several point mutations to this vector were created by site-directed mutagenesis.

Retroviral Plasmids: Human p110αH1047R was PCR amplified with the primers hp110αF-XhoI and hp110αR-HpaI, and the resulting fragment was digested with XhoI and HpaI and then ligated into the IRES-GFP retroviral vector pMIG to create pMIG-

p110α-H1047R. Several p110α point mutations to this vector were made by site-directed mutagenesis.

Murine Ecotropic Pseudotyping Vector: pcDNA3-EcoR plasmid DNA encoding the murine ecotropic receptor EcoR/MCAT-1 was a generous gift from Jeffrey Henise.

Primer Name	Primer Sequence (5'-3')
p110α-BamHI-NtermMyc-F	cttctggtaccatggaacagaaactcatatcggaggaggatctacctccacgaccatcatca ggtgaactgtgg
p110α-EcoRV-R	ccgcgatatctcagttcaatgcatgctgtttaattgtgtgg
hp110αF-XhoI	gtgctttgctcgagatgcctccacgaccatcatcaggtgaactg
hp110αR-HpaI	gtgcctcggttaactcagttcaatgcatgctgtttaattgtgtgg

Table 4.1. Oligonucleotide primers used for subcloning p110α.

4.4.2 In vitro PI3K kinase assays

pcDNA3-p110α plasmid DNA was transfected into HEK-293T cells with Lipofectamine 2000 (Invitrogen). After 48 hours the cells were trypsinized, washed with PBS, and pelleted for storage at -80°C. Pellets were lysed by vortexing in PI3K lysis buffer (50 mM Tris (pH 7.4), 300 mM NaCl, 5 mM EDTA, 0.02% NaN_3, 1% Triton X-100, protease inhibitor cocktail tablets (Roche), 8 mM sodium orthovanadate, 83 μM PMSF, 1X Phosphatase Inhibitor Cocktails 1 and 2 (Sigma)) and then immunoprecipitated by overnight incubation with Anti-c-Myc Agarose Affinity Gel (Sigma-Aldrich). The immunoprecipitates were washed with the following buffers: twice with buffer A (PBS, 1 mM EDTA, 1% Triton X-100), twice with buffer B (100 mM Tris pH 7.4, 500 mM LiCl, 1 mM EDTA), twice with buffer C (50 mM Tris pH 7.4, 100 mM NaCl), twice with PBS, and then assayed for PI3K activity in 96 well format essentially

as described [142]. Briefly, immunoprecipitated Myc-p110α was incubated "on bead" with shaking at 25°C with 100 μg/ml phosphatidylinositol, 10 μCi γ^{32}P-ATP, 10 μM ATP, 1 mg/ml BSA, 25 mM HEPES pH 7.4, 10 mM $MgCl_2$, 1:50 DMSO ± PI3K inhibitor. After 1 hour, 4 μl of each reaction was spotted onto a dry nitrocellulose membrane pre-rinsed with wash solution (1 M NaCl, 1% H_3PO_4). After the spots dried, the membrane was washed five times with wash solution, dried with a heat lamp, and exposed on a phosphor screen overnight. The phosphor screen was then scanned with a Typhoon phosphorimager (GE Healthcare) and the resulting data was quantified with the MATLAB script Spot [142].

4.4.3 MCF10A culture and transformation assays

MCF10A cells (ATCC) were cultured at 37°C, 5% CO_2 in MCF10A growth media (1:1 DMEM:F-12 supplemented with 5% filtered, heat inactivated horse serum, 20 ng/ml EGF, 100 μg/ml hydrocortisone, 1 ng/ml cholera toxin, 10 μg/ml insulin, and penicillin/streptomycin) as described [143].

4.4.4 Creation of p110α-expressing MCF10A cell lines

Mutant p110α expressing MCF10A lines were created by retroviral infection. Ecotropic p110α viral stocks were made by transfecting pMIG-p110α plasmid DNA into the Phoenix Eco cell line. Retroviral supernatants were collected at 48, 72, 96, and 120 hours, spun at 500 RPM for 5 minutes at 4°C, and stored in 0.5 ml aliquots at -80°C.

Human MCF10A cells were pseudotyped for infection with murine ecotropic virus by transient transfection with pcDNA3-EcoR/MCAT1. Transfection was performed by nucleofection (Amaxa Nucleofector) following the manufacturer's instructions, and the transfected cells were plated into 6-well plates. 24 hours after nucleofection with pcDNA3-EcoR/MCAT1, the MCF10A cells were infected with thawed p110α viral stocks for 12 hours, switched to growth media for 6 hours, and then expanded into 75cm^2 flasks. After 3 days, the infected cells were FACS sorted for GFP expression.

4.4.5 MCF10A EGF-independent transformation assays

MCF10A cell lines were assayed for oncogenic transformation by their ability to grow in media lacking EGF. Cells were seeded into black sided, clear bottom, 96-well plates at 2 x 10^3 cells per well in 100 µl growth media. After 2 days, the cells were washed with PBS and then switched to 100 µl growth media lacking EGF. Cell proliferation was monitored every 2 days by incubation with resazurin (alamar blue). A stock solution of 120 µg/ml resazurin in PBS was added to the cells at 1:20, incubated for 2 hours at 37°C, 15 minutes at room temperature, and then assayed for fluorescence with an excitation wavelength of 520 nm and an emission wavelength of 590 nm. After fluorescence measurement, the resazurin containing media was replaced with 100 µl fresh growth media lacking EGF and the cells were returned to 37°C, 5% CO_2.

4.4.6 MCF10A western blotting

40-70% confluent MCF10A cultures were starved for 24 hours with MCF10A media lacking EGF and insulin, and then treated for 60 minutes with PI3K inhibitors or a

DMSO control. After 60 minutes, the cells were lysed with PI3K lysis buffer and subject to western blotting with antibodies purchased from Santa Cruz (anti-GFP) and Cell Signaling (all other antibodies) as directed by the supplier.

4.5 Conclusion

The advent of high throughput screening and the great success of imatinib led the pharmaceutical industry to focus on highly specific kinase inhibitors, but currently a multi-targeted approach is gaining acceptance [144, 145]. Inhibiting multiple targets can increase efficacy [83] and theoretically should decrease the likelihood of drug resistance, although no study to our knowledge has conclusively shown a reduced likelihood of clinical resistance with multi-targeted vs. highly specific drugs. My results with the MCF10A cell line show that multi-targeted inhibitors are not as susceptible to drug resistance by mutation of the single target p110α, especially when they target additional kinases in the PI3K signaling pathway.

PI-103 and BEZ-235 block PI3K signaling downstream of p110α by inhibiting mTOR, and PP-110 blocks PI3K signaling upstream of p110α by inhibiting RTKs. The ability of these three inhibitors to block p110αH1047R-dependent MCF10A growth is largely unaffected by p110α resistance mutations, suggesting that mutation of additional targets is required to confer drug resistance. The possibility of accumulating multiple resistance mutations in a single cancer cell seems unlikely, but slight growth advantages at each step may increase the odds of successive mutations, especially during prolonged treatment. The rate and probability of resistance mutation accumulation will be an

important area of study for multi-targeted drugs in cancer therapy, accessible by careful monitoring of clinical trials as well as mammalian tissue culture screens.

In contrast to the gatekeeper residue Ile 848, the residue Ile 800 of p110α is tolerant to mutations, at least two of which confer drug resistance: I800L and I800M. The resistance conferred by these mutations is smaller than observed for the T315I gatekeeper mutant of BCR-ABL, but comparable to most other mutations that confer clinical resistance to imatinib [110, 146]. This residue is a potential hotspot for clinical resistance to PI3K inhibitors; fortunately my screen has identified PW-12 and BEZ-235 as inhibitors that potently target the I800L mutant. The fact that I800L confers resistance to all other inhibitors, but sensitizes p110α to PW-12 and BEZ-235 suggests that these inhibitors share a similar binding mode that differs from other scaffolds near residue I800. There are several inhibitor-bound PI3K structures available, but the co-crystal structures of PW-12 and BEZ-235 have not been reported, so it is difficult to rationalize these trends. Interestingly, the residue corresponding to I800 in mTOR is also leucine, and mTOR is potently targeted by BEZ-235 [86].

The drug-sensitizing mutation L814C will be a valuable tool to study the effect of p110α inhibition in various biological systems, because there is no selective p110α inhibitor currently available. One possible concern with the L814C mutation is that its "sensitizing" effect may simply be due to the loss of enzymatic activity, but in vitro kinase assays reveal large shifts in IC_{50} values, and yeast serial dilution analysis and MCF10A transformation assays indicate that this mutant behaves similarly to wild-type in a cellular context, although it does show reduced Akt/PKB phosphorylation.

By focusing on a small subset of p110α residues that line the affinity pocket, I have identified a potential resistance hotspot at I800 that confers 5-30 fold resistance to most PI3K inhibitors. While this discovery should help guide the design of second-generation PI3K inhibitors, a more complete mutagenic screen of p110α will be necessary to uncover the full spectrum of resistance mutations.

Bibliography

1. Cantley, L.C., *The phosphoinositide 3-kinase pathway.* Science, 2002. **296**(5573): p. 1655-7.
2. Luo, J., B.D. Manning, and L.C. Cantley, *Targeting the PI3K-Akt pathway in human cancer: rationale and promise.* Cancer Cell, 2003. **4**(4): p. 257-62.
3. Stephens, L., R. Williams, and P. Hawkins, *Phosphoinositide 3-kinases as drug targets in cancer.* Curr Opin Pharmacol, 2005. **5**(4): p. 357-65.
4. Hennessy, B.T., et al., *Exploiting the PI3K/AKT pathway for cancer drug discovery.* Nat Rev Drug Discov, 2005. **4**(12): p. 988-1004.
5. Chang, H.W., et al., *Transformation of chicken cells by the gene encoding the catalytic subunit of PI 3-kinase.* Science, 1997. **276**(5320): p. 1848-50.
6. Samuels, Y., et al., *High frequency of mutations of the PIK3CA gene in human cancers.* Science, 2004. **304**(5670): p. 554.
7. Shaw, R.J. and L.C. Cantley, *Ras, PI(3)K and mTOR signalling controls tumour cell growth.* Nature, 2006. **441**(7092): p. 424-30.
8. Cully, M., et al., *Beyond PTEN mutations: the PI3K pathway as an integrator of multiple inputs during tumorigenesis.* Nat Rev Cancer, 2006. **6**(3): p. 184-92.
9. Brugge, J., M.C. Hung, and G.B. Mills, *A new mutational AKTivation in the PI3K pathway.* Cancer Cell, 2007. **12**(2): p. 104-7.
10. Gupta, S., et al., *Binding of ras to phosphoinositide 3-kinase p110alpha is required for ras-driven tumorigenesis in mice.* Cell, 2007. **129**(5): p. 957-68.

11. Lim, K.H. and C.M. Counter, *Reduction in the requirement of oncogenic Ras signaling to activation of PI3K/AKT pathway during tumor maintenance.* Cancer Cell, 2005. **8**(5): p. 381-92.

12. Ward, S.G. and P. Finan, *Isoform-specific phosphoinositide 3-kinase inhibitors as therapeutic agents.* Curr Opin Pharmacol, 2003. **3**(4): p. 426-34.

13. Marone, R., et al., *Targeting phosphoinositide 3-kinase: moving towards therapy.* Biochim Biophys Acta, 2008. **1784**(1): p. 159-85.

14. Emmelot, P., et al., *Isolation of plasma membranes from rat and mouse livers and hepatomas.* Methods Enzymol, 1974. **31**(Pt A): p. 75-90.

15. Klenk, H.D. and P.W. Choppin, *Lipids of plasma membranes of monkey and hamster kidney cells and of parainfluenza virions grown in these cells.* Virology, 1969. **38**(2): p. 255-68.

16. Ray, T.K., et al., *Lipid composition of rat liver plasma membranes.* J Biol Chem, 1969. **244**(20): p. 5528-36.

17. Thom, D., et al., *Rapid isolation of plasma membranes in high yield from cultured fibroblasts.* Biochem J, 1977. **168**(2): p. 187-94.

18. Fruman, D.A., R.E. Meyers, and L.C. Cantley, *Phosphoinositide kinases.* Annu Rev Biochem, 1998. **67**: p. 481-507.

19. Mitchell, K.T., J.E. Ferrell, Jr., and W.H. Huestis, *Separation of phosphoinositides and other phospholipids by two-dimensional thin-layer chromatography.* Anal Biochem, 1986. **158**(2): p. 447-53.

20. Knight, Z.A., et al., *A pharmacological map of the PI3-K family defines a role for p110alpha in insulin signaling.* Cell, 2006. **125**(4): p. 733-47.

21. Hilgemann, D.W., S. Feng, and C. Nasuhoglu, *The complex and intriguing lives of PIP2 with ion channels and transporters.* Sci STKE, 2001. **2001**(111): p. RE19.

22. Streb, H., et al., *Release of Ca2+ from a nonmitochondrial intracellular store in pancreatic acinar cells by inositol-1,4,5-trisphosphate.* Nature, 1983. **306**(5938): p. 67-9.

23. Nishizuka, Y., *Turnover of inositol phospholipids and signal transduction.* Science, 1984. **225**(4668): p. 1365-70.

24. Fruman, D.A., L.E. Rameh, and L.C. Cantley, *Phosphoinositide binding domains: embracing 3-phosphate.* Cell, 1999. **97**(7): p. 817-20.

25. Stephens, L.R., K.T. Hughes, and R.F. Irvine, *Pathway of phosphatidylinositol(3,4,5)-trisphosphate synthesis in activated neutrophils.* Nature, 1991. **351**(6321): p. 33-9.

26. Escobedo, J.A., et al., *cDNA cloning of a novel 85 kd protein that has SH2 domains and regulates binding of PI3-kinase to the PDGF beta-receptor.* Cell, 1991. **65**(1): p. 75-82.

27. Myers, M.G., Jr., et al., *IRS-1 activates phosphatidylinositol 3'-kinase by associating with src homology 2 domains of p85.* Proc Natl Acad Sci U S A, 1992. **89**(21): p. 10350-4.

28. Stephens, L.R., et al., *The G beta gamma sensitivity of a PI3K is dependent upon a tightly associated adaptor, p101.* Cell, 1997. **89**(1): p. 105-14.

29. Suire, S., et al., *p84, a new Gbetagamma-activated regulatory subunit of the type IB phosphoinositide 3-kinase p110gamma.* Curr Biol, 2005. **15**(6): p. 566-70.

30. Voigt, P., M.B. Dorner, and M. Schaefer, *Characterization of p87PIKAP, a novel regulatory subunit of phosphoinositide 3-kinase gamma that is highly expressed in heart and interacts with PDE3B.* J Biol Chem, 2006. **281**(15): p. 9977-86.

31. Stoyanov, B., et al., *Cloning and characterization of a G protein-activated human phosphoinositide-3 kinase.* Science, 1995. **269**(5224): p. 690-3.

32. Guillermet-Guibert, J., et al., *The p110beta isoform of phosphoinositide 3-kinase signals downstream of G protein-coupled receptors and is functionally redundant with p110gamma.* Proc Natl Acad Sci U S A, 2008. **105**(24): p. 8292-7.

33. Rodriguez-Viciana, P., et al., *Activation of phosphoinositide 3-kinase by interaction with Ras and by point mutation.* Embo J, 1996. **15**(10): p. 2442-51.

34. Huang, C.H., et al., *The structure of a human p110alpha/p85alpha complex elucidates the effects of oncogenic PI3Kalpha mutations.* Science, 2007. **318**(5857): p. 1744-8.

35. Virbasius, J.V., A. Guilherme, and M.P. Czech, *Mouse p170 is a novel phosphatidylinositol 3-kinase containing a C2 domain.* J Biol Chem, 1996. **271**(23): p. 13304-7.

36. Falasca, M. and T. Maffucci, *Role of class II phosphoinositide 3-kinase in cell signalling.* Biochem Soc Trans, 2007. **35**(Pt 2): p. 211-4.

37. Backer, J.M., *The regulation and function of Class III PI3Ks: novel roles for Vps34.* Biochem J, 2008. **410**(1): p. 1-17.

38. Sugimoto, Y., et al., *Evidence that the Rous sarcoma virus transforming gene product phosphorylates phosphatidylinositol and diacylglycerol.* Proc Natl Acad Sci U S A, 1984. **81**(7): p. 2117-21.

39. Macara, I.G., G.V. Marinetti, and P.C. Balduzzi, *Transforming protein of avian sarcoma virus UR2 is associated with phosphatidylinositol kinase activity: possible role in tumorigenesis.* Proc Natl Acad Sci U S A, 1984. **81**(9): p. 2728-32.

40. Whitman, M., et al., *Association of phosphatidylinositol kinase activity with polyoma middle-T competent for transformation.* Nature, 1985. **315**(6016): p. 239-42.

41. Kaplan, D.R., et al., *Phosphatidylinositol metabolism and polyoma-mediated transformation.* Proc Natl Acad Sci U S A, 1986. **83**(11): p. 3624-8.

42. Kaplan, D.R., et al., *Common elements in growth factor stimulation and oncogenic transformation: 85 kd phosphoprotein and phosphatidylinositol kinase activity.* Cell, 1987. **50**(7): p. 1021-9.

43. Auger, K.R., et al., *PDGF-dependent tyrosine phosphorylation stimulates production of novel polyphosphoinositides in intact cells.* Cell, 1989. **57**(1): p. 167-75.

44. Whitman, M., et al., *Evidence for two distinct phosphatidylinositol kinases in fibroblasts. Implications for cellular regulation.* Biochem J, 1987. **247**(1): p. 165-74.

45. Carpenter, C.L., et al., *Purification and characterization of phosphoinositide 3-kinase from rat liver.* J Biol Chem, 1990. **265**(32): p. 19704-11.

46. Hiles, I.D., et al., *Phosphatidylinositol 3-kinase: structure and expression of the 110 kd catalytic subunit.* Cell, 1992. **70**(3): p. 419-29.

47. Courtneidge, S.A. and A. Heber, *An 81 kd protein complexed with middle T antigen and pp60c-src: a possible phosphatidylinositol kinase.* Cell, 1987. **50**(7): p. 1031-7.

48. Fukui, Y. and H. Hanafusa, *Phosphatidylinositol kinase activity associates with viral p60src protein.* Mol Cell Biol, 1989. **9**(4): p. 1651-8.

49. Varticovski, L., et al., *The colony stimulating factor-1 receptor associates with and activates phosphatidylinositol-3 kinase.* Nature, 1989. **342**(6250): p. 699-702.

50. Ikenoue, T., et al., *Functional analysis of PIK3CA gene mutations in human colorectal cancer.* Cancer Res, 2005. **65**(11): p. 4562-7.

51. Zhao, J.J., et al., *The oncogenic properties of mutant p110alpha and p110beta phosphatidylinositol 3-kinases in human mammary epithelial cells.* Proc Natl Acad Sci U S A, 2005. **102**(51): p. 18443-8.

52. Samuels, Y., et al., *Mutant PIK3CA promotes cell growth and invasion of human cancer cells.* Cancer Cell, 2005. **7**(6): p. 561-73.

53. Isakoff, S.J., et al., *Breast cancer-associated PIK3CA mutations are oncogenic in mammary epithelial cells.* Cancer Res, 2005. **65**(23): p. 10992-1000.

54. Kang, S., A.G. Bader, and P.K. Vogt, *Phosphatidylinositol 3-kinase mutations identified in human cancer are oncogenic.* Proc Natl Acad Sci U S A, 2005. **102**(3): p. 802-7.

55. Miled, N., et al., *Mechanism of two classes of cancer mutations in the phosphoinositide 3-kinase catalytic subunit.* Science, 2007. **317**(5835): p. 239-42.

56. Zhao, L. and P.K. Vogt, *Helical domain and kinase domain mutations in p110alpha of phosphatidylinositol 3-kinase induce gain of function by different mechanisms.* Proc Natl Acad Sci U S A, 2008. **105**(7): p. 2652-7.

57. Kang, S., et al., *Oncogenic transformation induced by the p110beta, -gamma, and -delta isoforms of class I phosphoinositide 3-kinase.* Proc Natl Acad Sci U S A, 2006. **103**(5): p. 1289-94.

58. Ciraolo, E., et al., *Phosphoinositide 3-kinase p110beta activity: key role in metabolism and mammary gland cancer but not development.* Sci Signal, 2008. **1**(36): p. ra3.

59. Torbett, N.E., et al., *A chemical screen in diverse breast cancer cell lines reveals genetic enhancers and suppressors of sensitivity to PI3K isoform-selective inhibition.* Biochem J, 2008. **415**(1): p. 97-110.

60. Wee, S., et al., *PTEN-deficient cancers depend on PIK3CB.* Proc Natl Acad Sci U S A, 2008. **105**(35): p. 13057-62.

61. Jia, S., et al., *Essential roles of PI(3)K-p110beta in cell growth, metabolism and tumorigenesis.* Nature, 2008. **454**(7205): p. 776-9.

62. Sujobert, P., et al., *Essential role for the p110delta isoform in phosphoinositide 3-kinase activation and cell proliferation in acute myeloid leukemia.* Blood, 2005. **106**(3): p. 1063-6.

63. Billottet, C., et al., *A selective inhibitor of the p110delta isoform of PI 3-kinase inhibits AML cell proliferation and survival and increases the cytotoxic effects of VP16.* Oncogene, 2006. **25**(50): p. 6648-59.

64. Hickey, F.B. and T.G. Cotter, *BCR-ABL regulates phosphatidylinositol 3-kinase-p110gamma transcription and activation and is required for proliferation and drug resistance.* J Biol Chem, 2006. **281**(5): p. 2441-50.

65. Sadhu, C., et al., *Essential role of phosphoinositide 3-kinase delta in neutrophil directional movement.* J Immunol, 2003. **170**(5): p. 2647-54.

66. Matter, W.F., R.F. Brown, and C.J. Vlahos, *The inhibition of phosphatidylinositol 3-kinase by quercetin and analogs.* Biochem Biophys Res Commun, 1992. **186**(2): p. 624-31.

67. Levy, J., et al., *Tyrosine protein kinase activity in the DMBA-induced rat mammary tumor: inhibition by quercetin.* Biochem Biophys Res Commun, 1984. **123**(3): p. 1227-33.

68. Graziani, Y., E. Erikson, and R.L. Erikson, *The effect of quercetin on the phosphorylation activity of the Rous sarcoma virus transforming gene product in vitro and in vivo.* Eur J Biochem, 1983. **135**(3): p. 583-9.

69. Cochet, C., et al., *Selective inhibition of a cyclic nucleotide independent protein kinase (G type casein kinase) by quercetin and related polyphenols.* Biochem Pharmacol, 1982. **31**(7): p. 1357-61.

70. Gschwendt, M., et al., *Inhibition of the calcium- and phospholipid-dependent protein kinase activity from mouse brain cytosol by quercetin.* Biochem Biophys Res Commun, 1983. **117**(2): p. 444-7.

71. Srivastava, A.K., *Inhibition of phosphorylase kinase, and tyrosine protein kinase activities by quercetin.* Biochem Biophys Res Commun, 1985. **131**(1): p. 1-5.

72. Vlahos, C.J., et al., *A specific inhibitor of phosphatidylinositol 3-kinase, 2-(4-morpholinyl)-8-phenyl-4H-1-benzopyran-4-one (LY294002).* J Biol Chem, 1994. **269**(7): p. 5241-8.

73. Brian, P.W., et al., *Wortmannin, an antibiotic produced by Penicillium wortmanni.* Trans. Br. Mycol. Soc., 1957. **40**: p. 365-368.

74. Arcaro, A. and M.P. Wymann, *Wortmannin is a potent phosphatidylinositol 3-kinase inhibitor: the role of phosphatidylinositol 3,4,5-trisphosphate in neutrophil responses.* Biochem J, 1993. **296 (Pt 2)**: p. 297-301.

75. Baggiolini, M., et al., *Inhibition of the phagocytosis-induced respiratory burst by the fungal metabolite wortmannin and some analogues.* Exp Cell Res, 1987. **169**(2): p. 408-18.

76. Brunn, G.J., et al., *Direct inhibition of the signaling functions of the mammalian target of rapamycin by the phosphoinositide 3-kinase inhibitors, wortmannin and LY294002.* Embo J, 1996. **15**(19): p. 5256-67.

77. Sarkaria, J.N., et al., *Inhibition of phosphoinositide 3-kinase related kinases by the radiosensitizing agent wortmannin.* Cancer Res, 1998. **58**(19): p. 4375-82.

78. Yuan, T.L. and L.C. Cantley, *PI3K pathway alterations in cancer: variations on a theme.* Oncogene, 2008. **27**(41): p. 5497-510.

79. Rommel, C., M. Camps, and H. Ji, *PI3K delta and PI3K gamma: partners in crime in inflammation in rheumatoid arthritis and beyond?* Nat Rev Immunol, 2007. **7**(3): p. 191-201.

80. Jackson, S.P., et al., *PI 3-kinase p110beta: a new target for antithrombotic therapy.* Nat Med, 2005. **11**(5): p. 507-14.

81. Barber, D.F., et al., *PI3Kgamma inhibition blocks glomerulonephritis and extends lifespan in a mouse model of systemic lupus.* Nat Med, 2005. **11**(9): p. 933-5.

82. Camps, M., et al., *Blockade of PI3Kgamma suppresses joint inflammation and damage in mouse models of rheumatoid arthritis.* Nat Med, 2005. **11**(9): p. 936-43.

83. Fan, Q.W., et al., *A dual PI3 kinase/mTOR inhibitor reveals emergent efficacy in glioma.* Cancer Cell, 2006. **9**(5): p. 341-9.

84. Hayakawa, M., et al., *Synthesis and biological evaluation of imidazo[1,2-a]pyridine derivatives as novel PI3 kinase p110alpha inhibitors.* Bioorg Med Chem, 2007. **15**(1): p. 403-12.

85. Apsel, B., et al., *Targeted polypharmacology: discovery of dual inhibitors of tyrosine and phosphoinositide kinases.* Nat Chem Biol, 2008. **4**(11): p. 691-9.

86. Stauffer, F., et al., *Imidazo[4,5-c]quinolines as inhibitors of the PI3K/PKB-pathway.* Bioorg Med Chem Lett, 2008. **18**(3): p. 1027-30.

87. Walker, E.H., et al., *Structural insights into phosphoinositide 3-kinase catalysis and signalling.* Nature, 1999. **402**(6759): p. 313-20.

88. Weiss, W.A., S.S. Taylor, and K.M. Shokat, *Recognizing and exploiting differences between RNAi and small-molecule inhibitors.* Nat Chem Biol, 2007. **3**(12): p. 739-44.

89. Schindler, T., et al., *Structural mechanism for STI-571 inhibition of abelson tyrosine kinase.* Science, 2000. **289**(5486): p. 1938-42.

90. Wan, P.T., et al., *Mechanism of activation of the RAF-ERK signaling pathway by oncogenic mutations of B-RAF.* Cell, 2004. **116**(6): p. 855-67.

91. Ohren, J.F., et al., *Structures of human MAP kinase kinase 1 (MEK1) and MEK2 describe novel noncompetitive kinase inhibition.* Nat Struct Mol Biol, 2004. **11**(12): p. 1192-7.

92. Lindsley, C.W., et al., *Allosteric Akt (PKB) inhibitors: discovery and SAR of isozyme selective inhibitors.* Bioorg Med Chem Lett, 2005. **15**(3): p. 761-4.

93. Karaman, M.W., et al., *A quantitative analysis of kinase inhibitor selectivity.* Nat Biotechnol, 2008. **26**(1): p. 127-32.

94. Godl, K., et al., *An efficient proteomics method to identify the cellular targets of protein kinase inhibitors.* Proc Natl Acad Sci U S A, 2003. **100**(26): p. 15434-9.

95. Cohen, M.S., et al., *Structural bioinformatics-based design of selective, irreversible kinase inhibitors.* Science, 2005. **308**(5726): p. 1318-21.

96. Bishop, A.C., et al., *A chemical switch for inhibitor-sensitive alleles of any protein kinase.* Nature, 2000. **407**(6802): p. 395-401.

97. Chen, X., et al., *A chemical-genetic approach to studying neurotrophin signaling.* Neuron, 2005. **46**(1): p. 13-21.

98. Larochelle, S., et al., *Requirements for Cdk7 in the assembly of Cdk1/cyclin B and activation of Cdk2 revealed by chemical genetics in human cells.* Mol Cell, 2007. **25**(6): p. 839-50.

99. Kohli, M., et al., *Facile methods for generating human somatic cell gene knockouts using recombinant adeno-associated viruses.* Nucleic Acids Res, 2004. **32**(1): p. e3.

100. Rago, C., B. Vogelstein, and F. Bunz, *Genetic knockouts and knockins in human somatic cells.* Nat Protoc, 2007. **2**(11): p. 2734-46.

101. Shah, K., et al., *Engineering unnatural nucleotide specificity for Rous sarcoma virus tyrosine kinase to uniquely label its direct substrates.* Proc Natl Acad Sci U S A, 1997. **94**(8): p. 3565-70.

102. Blethrow, J.D., et al., *Covalent capture of kinase-specific phosphopeptides reveals Cdk1-cyclin B substrates.* Proc Natl Acad Sci U S A, 2008. **105**(5): p. 1442-7.

103. Allen, J.J., S.E. Lazerwith, and K.M. Shokat, *Bio-orthogonal affinity purification of direct kinase substrates.* J Am Chem Soc, 2005. **127**(15): p. 5288-9.

104. Daub, H., K. Specht, and A. Ullrich, *Strategies to overcome resistance to targeted protein kinase inhibitors.* Nat Rev Drug Discov, 2004. **3**(12): p. 1001-10.

105. Carter, T.A., et al., *Inhibition of drug-resistant mutants of ABL, KIT, and EGF receptor kinases.* Proc Natl Acad Sci U S A, 2005. **102**(31): p. 11011-6.

106. Alaimo, P.J., Z.A. Knight, and K.M. Shokat, *Targeting the gatekeeper residue in phosphoinositide 3-kinases.* Bioorg Med Chem, 2005. **13**(8): p. 2825-36.

107. Shah, N.P., et al., *Overriding imatinib resistance with a novel ABL kinase inhibitor.* Science, 2004. **305**(5682): p. 399-401.

108. Quintas-Cardama, A., H. Kantarjian, and J. Cortes, *Flying under the radar: the new wave of BCR-ABL inhibitors.* Nat Rev Drug Discov, 2007. **6**(10): p. 834-48.

109. Azam, M., R.R. Latek, and G.Q. Daley, *Mechanisms of autoinhibition and STI-571/imatinib resistance revealed by mutagenesis of BCR-ABL.* Cell, 2003. **112**(6): p. 831-43.

110. von Bubnoff, N., et al., *A cell-based screen for resistance of Bcr-Abl-positive leukemia identifies the mutation pattern for PD166326, an alternative Abl kinase inhibitor.* Blood, 2005. **105**(4): p. 1652-9.

111. Engelman, J.A., et al., *Allelic dilution obscures detection of a biologically significant resistance mutation in EGFR-amplified lung cancer.* J Clin Invest, 2006. **116**(10): p. 2695-706.

112. Odorizzi, G., M. Babst, and S.D. Emr, *Phosphoinositide signaling and the regulation of membrane trafficking in yeast.* Trends Biochem Sci, 2000. **25**(5): p. 229-35.

113. Tugendreich, S., et al., *A streamlined process to phenotypically profile heterologous cDNAs in parallel using yeast cell-based assays.* Genome Res, 2001. **11**(11): p. 1899-912.

114. Rodriguez-Escudero, I., et al., *Reconstitution of the mammalian PI3K/PTEN/Akt pathway in yeast.* Biochem J, 2005. **390**(Pt 2): p. 613-23.

115. Audhya, A., et al., *Genome-wide lethality screen identifies new PI4,5P2 effectors that regulate the actin cytoskeleton.* Embo J, 2004. **23**(19): p. 3747-57.

116. Casamayor, A. and M. Snyder, *Molecular dissection of a yeast septin: distinct domains are required for septin interaction, localization, and function.* Mol Cell Biol, 2003. **23**(8): p. 2762-77.

117. Andres-Pons, A., et al., *In vivo functional analysis of the counterbalance of hyperactive phosphatidylinositol 3-kinase p110 catalytic oncoproteins by the tumor suppressor PTEN.* Cancer Res, 2007. **67**(20): p. 9731-9.

118. Gray, N.S., et al., *Exploiting chemical libraries, structure, and genomics in the search for kinase inhibitors.* Science, 1998. **281**(5376): p. 533-8.

119. Gaber, R.F., et al., *The yeast gene ERG6 is required for normal membrane function but is not essential for biosynthesis of the cell-cycle-sparking sterol.* Mol Cell Biol, 1989. **9**(8): p. 3447-56.

120. Leppert, G., et al., *Cloning by gene amplification of two loci conferring multiple drug resistance in Saccharomyces.* Genetics, 1990. **125**(1): p. 13-20.

121. Decottignies, A., et al., *Identification and characterization of SNQ2, a new multidrug ATP binding cassette transporter of the yeast plasma membrane.* J Biol Chem, 1995. **270**(30): p. 18150-7.

122. Cutler, N.S., J. Heitman, and M.E. Cardenas, *STT4 is an essential phosphatidylinositol 4-kinase that is a target of wortmannin in Saccharomyces cerevisiae.* J Biol Chem, 1997. **272**(44): p. 27671-7.

123. Camonis, J.H. and M. Jacquet, *A new RAS mutation that suppresses the CDC25 gene requirement for growth of Saccharomyces cerevisiae.* Mol Cell Biol, 1988. **8**(7): p. 2980-3.

124. Taparowsky, E., et al., *Structure and activation of the human N-ras gene.* Cell, 1983. **34**(2): p. 581-6.

125. Isakoff, S.J., et al., *Identification and analysis of PH domain-containing targets of phosphatidylinositol 3-kinase using a novel in vivo assay in yeast.* Embo J, 1998. **17**(18): p. 5374-87.

126. Yu, J., et al., *Regulation of the p85/p110 phosphatidylinositol 3'-kinase: stabilization and inhibition of the p110alpha catalytic subunit by the p85 regulatory subunit.* Mol Cell Biol, 1998. **18**(3): p. 1379-87.

127. Mumberg, D., R. Muller, and M. Funk, *Yeast vectors for the controlled expression of heterologous proteins in different genetic backgrounds.* Gene, 1995. **156**(1): p. 119-22.

128. Lamprecht, M.R., D.M. Sabatini, and A.E. Carpenter, *CellProfiler: free, versatile software for automated biological image analysis.* Biotechniques, 2007. **42**(1): p. 71-5.

129. Balla, A., et al., *Design of drug-resistant alleles of type-III phosphatidylinositol 4-kinases using mutagenesis and molecular modeling.* Biochemistry, 2008. **47**(6): p. 1599-607.

130. Rodgers, E.E. and A.B. Theibert, *Functions of PI 3-kinase in development of the nervous system.* Int J Dev Neurosci, 2002. **20**(3-5): p. 187-97.

131. Cosker, K.E. and B.J. Eickholt, *Phosphoinositide 3-kinase signalling events controlling axonal morphogenesis.* Biochem Soc Trans, 2007. **35**(Pt 2): p. 207-10.

132. Kwon, C.H., et al., *Pten regulates neuronal arborization and social interaction in mice.* Neuron, 2006. **50**(3): p. 377-88.

133. Hale, B.G. and R.E. Randall, *PI3K signalling during influenza A virus infections.* Biochem Soc Trans, 2007. **35**(Pt 2): p. 186-7.

134. Paling, N.R., et al., *Regulation of embryonic stem cell self-renewal by phosphoinositide 3-kinase-dependent signaling.* J Biol Chem, 2004. **279**(46): p. 48063-70.

135. Boschelli, D.H., et al., *Synthesis and Src kinase inhibitory activity of a series of 4-phenylamino-3-quinolinecarbonitriles.* J Med Chem, 2001. **44**(5): p. 822-33.

136. Brugge, J.S., et al., *Expression of Rous sarcoma virus transforming protein pp60v-src in Saccharomyces cerevisiae cells.* Mol Cell Biol, 1987. **7**(6): p. 2180-7.

137. Nakayama, G.R., et al., *Assessment of the Alamar Blue assay for cellular growth and viability in vitro.* J Immunol Methods, 1997. **204**(2): p. 205-8.

138. O'Brien, J., et al., *Investigation of the Alamar Blue (resazurin) fluorescent dye for the assessment of mammalian cell cytotoxicity.* Eur J Biochem, 2000. **267**(17): p. 5421-6.

139. Hayakawa, M., et al., *Synthesis and biological evaluation of pyrido[3',2':4,5]furo[3,2-d]pyrimidine derivatives as novel PI3 kinase p110alpha inhibitors.* Bioorg Med Chem Lett, 2007. **17**(9): p. 2438-42.

140. Raynaud, F.I., et al., *Pharmacologic characterization of a potent inhibitor of class I phosphatidylinositide 3-kinases.* Cancer Res, 2007. **67**(12): p. 5840-50.

141. Sarbassov, D.D., et al., *Phosphorylation and regulation of Akt/PKB by the rictor-mTOR complex.* Science, 2005. **307**(5712): p. 1098-101.

142. Knight, Z.A., et al., *A membrane capture assay for lipid kinase activity.* Nat Protoc, 2007. **2**(10): p. 2459-66.

143. Debnath, J., S.K. Muthuswamy, and J.S. Brugge, *Morphogenesis and oncogenesis of MCF-10A mammary epithelial acini grown in three-dimensional basement membrane cultures.* Methods, 2003. **30**(3): p. 256-68.

144. Branca, M.A., *Multi-kinase inhibitors create buzz at ASCO.* Nat Biotechnol, 2005. **23**(6): p. 639.

145. Jimeno, A. and M. Hidalgo, *Multitargeted therapy: can promiscuity be praised in an era of political correctness?* Crit Rev Oncol Hematol, 2006. **59**(2): p. 150-8.

146. Shah, N.P., et al., *Multiple BCR-ABL kinase domain mutations confer polyclonal resistance to the tyrosine kinase inhibitor imatinib (STI571) in chronic phase and blast crisis chronic myeloid leukemia.* Cancer Cell, 2002. **2**(2): p. 117-25.

Publishing Agreement

It is the policy of the University to encourage the distribution of all theses, dissertations, and manuscripts. Copies of all UCSF theses, dissertations, and manuscripts will be routed to the library via the Graduate Division. The library will make all theses, dissertations, and manuscripts accessible to the public and will preserve these to the best of their abilities, in perpetuity.

Please sign the following statement:

I hereby grant permission to the Graduate Division of the University of California, San Francisco to release copies of my thesis, dissertation, or manuscript to the Campus Library to provide access and preservation, in whole or in part, in perpetuity.

Eli Zunder

Author Signature

1/8/2009

Date